



# Radiative leptonic $B_c \rightarrow \gamma \ell \bar{\nu}$ decay in effective field theory beyond leading order

Wei Wang<sup>1,2,a</sup>, Rui-Lin Zhu<sup>1,2,b</sup><sup>1</sup> INPAC, Shanghai Key Laboratory for Particle Physics and Cosmology, Department of Physics and Astronomy, Shanghai Jiao Tong University, Shanghai 200240, China<sup>2</sup> State Key Laboratory of Theoretical Physics, Institute of Theoretical Physics, Chinese Academy of Sciences, Beijing 100190, ChinaReceived: 6 April 2015 / Accepted: 27 July 2015 / Published online: 8 August 2015  
© The Author(s) 2015. This article is published with open access at [Springerlink.com](http://Springerlink.com)

**Abstract** We study the radiative leptonic  $B_c \rightarrow \gamma \ell \bar{\nu}$  decays in nonrelativistic QCD effective field theory, and we explore the contribution from a fast-moving photon. As a result, interactions between the photon and the heavy quarks can be integrated out, resulting in the factorization formula for the decay amplitude. We calculate not only the relevant short-distance coefficients at leading order and next-to-leading order in  $\alpha_s$ , but also the nonrelativistic corrections at the order  $|v|^2$  in our analysis. We find that the QCD corrections can significantly decrease the branching ratio, and this is of great importance in extracting the long-distance operator matrix elements of  $B_c$ . For phenomenological application, we present our results for the photon energy, lepton energy and lepton-neutrino invariant mass distribution.

## 1 Introduction

The search for new degrees of freedom may proceed in two distinctive directions. At the high energy frontier, new particles have different signatures from the standard model (SM) particles, and measurements of their production may provide definitive evidence of their existence. On the other hand, it is likely that low energy processes will be influenced through loop effects. Rare decays of heavy mesons, with tiny decay rates in the SM, are sensitive to the new degrees of freedom and thus can be exploited as indirect searches of these unknown effects; for a recent review see Ref. [1].

The  $B_c$  meson is the unique pseudo-scalar meson that is long lived and composed of two different heavy flavors. Since this hadron is stable against strong interactions, its weak decays provide rich phenomena for the study of CKM matrix elements and also a platform to study the effects of

weak interactions in a heavy quarkonium system [2,3]. In the past decades it has received growing attention since the first observation by the CDF Collaboration [4]. This is particularly shown by the recent LHCb measurements of the  $B_c$  lifetime [5,6], the decay widths of  $B_c \rightarrow J/\psi \pi$  and  $B_c \rightarrow J/\psi \ell \bar{\nu}$  [7,8], and various other decay modes [9–12]. One may expect that more decay channels of  $B_c$  can be measured by the LHCb, ATLAS, and CMS experiments [13–15].

On the theoretical side, various approaches have been applied to calculation of the decay width of  $B_c$  decays [16–52], but most of them are phenomenological. Since both constituents of the  $B_c$  are heavy and can only be treated nonrelativistically, an effective field theory can be established [53]. Taking the  $B_c \rightarrow J/\psi \ell \bar{\nu}$  as an example, one has the conjectured factorization formula in nonrelativistic QCD (NRQCD) for its decay amplitude [39,46,47]

$$\mathcal{A}(B_c \rightarrow J/\psi) \propto C_{ij} \langle 0 | \mathcal{O}_i^{\bar{c}b} | \bar{B}_c \rangle \times \langle J/\psi | \mathcal{O}_j^{\bar{c}c} | 0 \rangle, \quad (1)$$

where the  $\mathcal{O}_{i,j}^{ff'}$  are constructed by low energy operators. The short-distance, or *hard*, contributions at the length scale  $1/m_{b,c}$  are encapsulated by the coefficients  $C_{ij}$ , which can be computed in perturbation theory. It is necessary to stress that a proof of the above factorization in Eq. (1) is not available.

The long-distance, or *soft*, part of the matrix elements have to be extracted in a non-perturbative approach, for instance the lattice QCD simulation, or these have to be constrained by much simpler processes, for instance the annihilation modes  $B_c \rightarrow \ell \bar{\nu}$  and  $B_c \rightarrow \gamma \ell \bar{\nu}$ . However, the usefulness of the  $B_c \rightarrow \ell \bar{\nu}$  is challenged in two respects. First, its decay rate is given by

$$\Gamma(B_c \rightarrow \ell \bar{\nu}) = \frac{G_F^2}{8\pi} |V_{cb}|^2 f_{B_c}^2 m_{B_c}^3 \frac{m_\ell^2}{m_{B_c}^2} \left( 1 - \frac{m_\ell^2}{m_{B_c}^2} \right)^2, \quad (2)$$

<sup>a</sup> e-mail: [wei.wang@sjtu.edu.cn](mailto:wei.wang@sjtu.edu.cn)<sup>b</sup> e-mail: [rlzhu@sjtu.edu.cn](mailto:rlzhu@sjtu.edu.cn)

in which the suppression factor  $m_\ell^2/m_{B_c}^2$  arises from the helicity flip. As a result,  $B_c \rightarrow \mu \bar{\nu}_\mu$  and  $B_c \rightarrow e \bar{\nu}_e$  have tiny branching fractions, which may be beyond the detector capability at the current experimental facilities. Second, there is only one physical observable, namely the decay rate, and thus  $B_c \rightarrow \ell \bar{\nu}$  is not capable to uniquely determine all long-distance matrix elements (LDMEs), there being typically more than one when relativistic corrections are taken into account.

On the contrary,  $B_c \rightarrow \gamma \ell \bar{\nu}$  can provide a wealth of information [54–58] in terms of a number of observables ranging from the decay probabilities and polarizations, to an angular analysis. It is interesting to notice that the counterpart in  $B$  sector,  $B \rightarrow \gamma \ell \bar{\nu}$ , has been widely discussed as regards the understanding of the  $B$  meson light-cone distribution amplitudes [59–63]. The small branching fraction of  $B_c \rightarrow \gamma \ell \bar{\nu}$  can be compensated by the high luminosity at the ongoing hadron colliders and the experimental facilities under design. The main purpose of this paper is to explore  $B_c \rightarrow \gamma \ell \bar{\nu}$  at next-to-leading order (NLO) in  $\alpha_s$  and in  $|\mathbf{v}|^2$ , which shall catch up with the progress in  $B_c \rightarrow \ell \bar{\nu}$  [55, 64]. For the leptonic decay constant, the two-loop calculation is also available in Refs. [65, 66].

The rest of this paper is organized as follows. In Sect. 2, we will derive the formulas for the various partial decay widths of  $B_c \rightarrow \gamma \ell \bar{\nu}$ . Section 3 is devoted to an extensive next-to-leading order calculation. We will discuss the phenomenological results in Sect. 4. We summarize our findings and conclude in Sect. 5. We relegate the details of the calculation to the appendix.

## 2 $B_c \rightarrow \gamma \ell \bar{\nu}$

In the SM, leading-order (LO) Feynman diagrams for the  $B_c \rightarrow \gamma \ell \bar{\nu}$  decay are shown in Fig. 1. The photon emission from a virtual  $W$ -boson is suppressed by  $1/m_W^2$  compared to other contributions, and thus the second diagram in Fig. 1 can be neglected. Integrating out the off-shell  $W$ -boson, we arrive at the effective electro-weak Hamiltonian

$$H_{\text{eff}} = \frac{G_F}{\sqrt{2}} V_{cb} \bar{c} \gamma_\mu (1 - \gamma_5) b \bar{\ell} \gamma^\mu (1 - \gamma_5) \nu + \text{h.c.}, \quad (3)$$

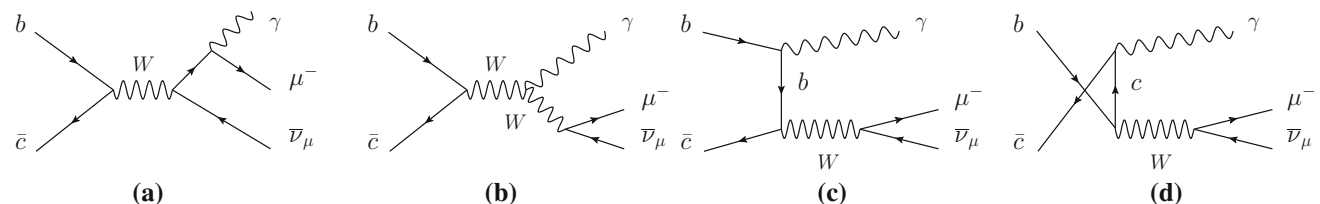


**Fig. 1** Leading-order Feynman diagrams for the radiative leptonic  $B_c \rightarrow \gamma \mu \bar{\nu}_\mu$  decay in the SM. The lepton  $\mu$  can also be  $e$  or  $\tau$ . The photon emission from a virtual  $W$ -boson, shown in the second panel, is suppressed by  $1/m_W^2$  compared to the other contributions

where  $V_{cb}$  is the CKM matrix element. The decay amplitude, the matrix element of the above Hamiltonian between the  $B_c$  and the  $\gamma \ell \bar{\nu}$  state,

$$\mathcal{A} = \langle \gamma \ell \bar{\nu} | H_{\text{eff}} | \bar{B}_c \rangle \quad (4)$$

is responsible for the process  $B_c \rightarrow \gamma \ell \bar{\nu}$ .

### 2.1 Differential decay widths

Since there is no strong interaction connection between the leptonic and the hadronic part, the decay amplitude can be decomposed into two individual sectors:

$$\mathcal{A} = \frac{G_F}{\sqrt{2}} V_{cb} \{ \langle 0 | \bar{c} \gamma_\mu (1 - \gamma_5) b | \bar{B}_c \rangle \times \langle \gamma \ell \bar{\nu} | \bar{\ell} \gamma^\mu (1 - \gamma_5) \nu | 0 \rangle + \langle \gamma | \bar{c} \gamma_\mu (1 - \gamma_5) b | \bar{B}_c \rangle \times \bar{u}_\ell \gamma^\mu (1 - \gamma_5) v_\nu \}, \quad (5)$$

with the matrix elements encoding the hadronic effects:

$$\langle 0 | \bar{c} \gamma_\mu (1 - \gamma_5) b | \bar{B}_c \rangle, \quad \langle \gamma | \bar{c} \gamma_\mu (1 - \gamma_5) b | \bar{B}_c \rangle. \quad (6)$$

The first one defines the  $B_c$  decay constant

$$\langle 0 | \bar{c} \gamma_\mu \gamma_5 b | \bar{B}_c(p_{B_c}) \rangle = i f_{B_c} p_{B_c, \mu}, \quad (7)$$

while the  $B_c \rightarrow \gamma$  transition is parametrized by two form factors:

$$\begin{aligned} \langle \gamma(\epsilon, k) | \bar{c} \gamma_\mu b | \bar{B}_c(p_{B_c}) \rangle &= -e \frac{V(L^2)}{p_{B_c} \cdot k} \epsilon_{\mu\nu\rho\sigma} \epsilon^{*\nu} p_{B_c}^\rho k^\sigma, \quad (8) \\ \langle \gamma(\epsilon, k) | \bar{c} \gamma_\mu \gamma_5 b | \bar{B}_c(p_{B_c}) \rangle &= i e A(L^2) \left( \epsilon_\mu^* - k_\mu \frac{p_{B_c} \cdot \epsilon^*}{p_{B_c} \cdot k} \right) \\ &\quad - \frac{i e}{p_{B_c} \cdot k} f_{B_c} p_{B_c, \mu} p_{B_c} \cdot \epsilon^*, \quad (9) \end{aligned}$$

with the momentum transfer  $L = p_{B_c} - k$ . Here and throughout this work we adopt the convention  $\epsilon^{0123} = +1$ . The above equations are similar to the parameterization of the  $B \rightarrow \gamma$  form factors as given in Ref. [67]. The last term in Eq. (9), which is proportional to the  $B_c$  decay constant, has been added in order to maintain the gauge invariance of the full amplitude [68, 69]; see Appendix A for a derivation.

Substituting Eqs. (7)–(9) into Eq. (5), we obtain

$$\mathcal{A} = -i \frac{G_F}{\sqrt{2}} V_{cb} e f_{B_c} \bar{u}_\ell \gamma^\mu (1 - \gamma_5) v_\nu \left\{ [1 + a(s_l)] \times \left( \epsilon_\mu^* - k_\mu \frac{p_{B_c} \cdot \epsilon^*}{p_{B_c} \cdot k} \right) - \frac{i v(s_l)}{p_{B_c} \cdot k} \epsilon_{\mu\nu\rho\sigma} \epsilon^{*\nu} p_{B_c}^\rho k^\sigma \right\}, \quad (10)$$

where  $s_l = L^2$  and terms due to lepton mass corrections have been neglected. Apparently, this expression is gauge invariant. For the sake of simplicity, we have defined two abbreviations in the above<sup>1</sup>

$$a(s_l) \equiv \frac{A(s_l)}{f_{B_c}}, \quad v(s_l) \equiv \frac{V(s_l)}{f_{B_c}}. \quad (11)$$

In terms of the decay constant and form factors, the differential decay width for the  $B_c \rightarrow \gamma \ell^- \bar{\nu}$  is given as

$$\begin{aligned} \frac{d^2\Gamma}{dE_k dE_l} &= \frac{1}{64m_{B_c}\pi^3} |\mathcal{A}|^2 \\ &= \frac{\alpha_{\text{em}} f_{B_c}^2 |V_{cb}|^2 G_F^2 m_{B_c}}{4\pi^2 x_k^2} (1 - x_k) \\ &\quad \times [a^2(x_k^2 + 2x_k(x_l - 1) + 2(x_l - 1)^2) \\ &\quad + 2a((v + 1)x_k^2 + 2(v + 1)x_k(x_l - 1) + 2(x_l - 1)^2) \\ &\quad + 2vx_k(x_k + 2x_l - 2) \\ &\quad + v^2(x_k^2 + 2x_k(x_l - 1) + 2(x_l - 1)^2) \\ &\quad + x_k^2 + 2x_k x_l - 2x_k + 2x_l^2 - 4x_l + 2], \end{aligned} \quad (12)$$

where  $x_k = 2E_k/m_{B_c}$  and  $y = 2E_l/m_{B_c}$ , and  $E_k$  and  $E_l$  are the energy of the photon and of the charged lepton in the  $B_c$  rest frame, respectively. One can integrate out  $E_l$  and obtain

$$\frac{d\Gamma}{dE_k} = \frac{\alpha_{\text{em}} f_{B_c}^2 |V_{cb}|^2 G_F^2 m_{B_c}^2 x_k (1 - x_k) ((1 + a)^2 + v^2)}{12\pi^2}. \quad (13)$$

The differential distributions can also be converted to

$$\begin{aligned} \frac{d^2\Gamma}{ds_l d\cos\theta_l} &= \frac{m_{B_c}^2 - s_l}{32m_{B_c}\pi^2} |V_{cb}|^2 \alpha_{\text{em}} f_{B_c}^2 G_F^2 (1 - x_k) \\ &\quad \times \frac{1}{x_k^2} [a^2(x_k^2 + 2x_k(x_l - 1) + 2(x_l - 1)^2) \\ &\quad + 2a((v + 1)x_k^2 + 2(v + 1)x_k(x_l - 1) + 2(x_l - 1)^2) \\ &\quad + 2vx_k(x_k + 2x_l - 2) + v^2(x_k^2 + 2x_k(x_l - 1) + 2(x_l - 1)^2) \\ &\quad + x_k^2 + 2x_k x_l - 2x_k + 2x_l^2 - 4x_l + 2], \end{aligned} \quad (14)$$

<sup>1</sup> One should distinguish the form factor  $v$  from the relative velocity  $v$  to be defined in the following.

using the relation

$$E_k = \frac{m_{B_c}^2 - s_l}{2m_{B_c}}, \quad (15)$$

$$E_l = \frac{1}{4m_{B_c}} [(m_{B_c}^2 + s_l) - (m_{B_c}^2 - s_l) \cos\theta_l]. \quad (16)$$

The  $\theta_l$  is the polar angle between the lepton  $\ell$  flight direction and the opposite direction of the  $B_c$  meson in the rest frame of the  $\ell\bar{\nu}_\ell$  pair. Likewise one can integrate out  $\theta_l$ ,

$$\frac{d\Gamma}{ds_l} = \frac{\alpha_{\text{em}} f_{B_c}^2 |V_{cb}|^2 G_F^2 (m_{B_c}^2 - s_l) s_l ((1 + a)^2 + v^2)}{24\pi^2 m_{B_c}^3}. \quad (17)$$

## 2.2 NRQCD factorization

The factorization properties for  $B_c \rightarrow \gamma \ell^- \bar{\nu}$  depend on the kinematics of the photon. In particular, the contribution from a soft photon,  $E_k \sim \Lambda_{\text{QCD}}$  with  $\Lambda_{\text{QCD}}$  being the hadronic scale, will introduce complexities as discussed for  $B$  decays in [70], and we will leave such a contribution for future work. Fortunately in the region where the photon is hadron, namely  $E_k \gg \Lambda_{\text{QCD}}$ , its interaction with heavy quarks is highly virtual and thus should be encoded in the short-distance coefficients. In the NRQCD scheme, we only need retain those color-singlet operator matrix elements that connect the  $B_c$  state to the vacuum. To the desired order, one expects the following factorization formula:

$$\begin{aligned} f_{B_c} &= \sqrt{\frac{2}{m_{B_c}}} \left[ c_0^f \langle 0 | \chi_c^\dagger \psi_b | \bar{B}_c(\mathbf{p}) \rangle \right. \\ &\quad \left. + \frac{c_2^f}{m_{B_c}^2} \left\langle 0 \left| \chi_c^\dagger \left( -\frac{i}{2} \overleftrightarrow{D} \right)^2 \psi_b \right| \bar{B}_c(\mathbf{p}) \right\rangle + \mathcal{O}(v^4) \right], \end{aligned} \quad (18)$$

$$\begin{aligned} V &= \sqrt{\frac{2}{m_{B_c}}} \left[ \frac{c_0^V}{m_{B_c}} \langle 0 | \chi_c^\dagger \psi_b | \bar{B}_c(\mathbf{p}) \rangle \right. \\ &\quad \left. + \frac{c_2^V}{m_{B_c}^3} \left\langle 0 \left| \chi_c^\dagger \left( -\frac{i}{2} \overleftrightarrow{D} \right)^2 \psi_b \right| \bar{B}_c(\mathbf{p}) \right\rangle + \mathcal{O}(v^4) \right], \end{aligned} \quad (19)$$

$$\begin{aligned} A &= \sqrt{\frac{2}{m_{B_c}}} \left[ \frac{c_0^A}{m_{B_c}} \langle 0 | \chi_c^\dagger \psi_b | \bar{B}_c(\mathbf{p}) \rangle \right. \\ &\quad \left. + \frac{c_2^A}{m_{B_c}^3} \left\langle 0 \left| \chi_c^\dagger \left( -\frac{i}{2} \overleftrightarrow{D} \right)^2 \psi_b \right| \bar{B}_c(\mathbf{p}) \right\rangle + \mathcal{O}(v^4) \right], \end{aligned} \quad (20)$$

where  $v$  denotes half the relative velocity between the charm and bottom quarks in the meson,  $c_0^{f,V,A}$  and  $c_2^{f,V,A}$  are the dimensionless short-distance coefficients, which can be

expanded in terms of the strong coupling constant.<sup>2</sup> We shall calculate the one-loop corrections to the  $c_0^{f,V,A}$ , but we give only the LO results for  $c_2^{f,V,A}$  since the latter ones are already power-suppressed.  $\psi_Q$  and  $\chi_Q^\dagger$  represent Pauli spinor fields that annihilate the heavy quark  $Q$  and anti-quark  $\bar{Q}$ , respectively. Besides, one needs to note that the state  $|H(p)\rangle$  in QCD has the standard normalization:  $\langle H(p')|H(p)\rangle = 2E_p(2\pi)^3\delta^3(\mathbf{p}-\mathbf{p}')$ , while an additional factor  $2E_p$  is abandoned in the nonrelativistic normalization where  $\langle H(\mathbf{p}')|H(\mathbf{p})\rangle = (2\pi)^3\delta^3(\mathbf{p}-\mathbf{p}')$ .

### 3 Next-to-leading order calculation

#### 3.1 Kinematics

Let  $p_1$  and  $p_2$  represent the momenta for the heavy quark  $Q$  and anti-quark  $\bar{Q}'$ . Without loss of generality, one may adopt the decomposition:

$$p_1 = \alpha P_{B_c} - q, \quad (21)$$

$$p_2 = \beta P_{B_c} + q, \quad (22)$$

where  $P_{B_c}$  is the total momentum of the quark pair.  $q$  is half of the relative momentum between the quark pair with  $P_{B_c} \cdot q = 0$ .  $\alpha$  and  $\beta$  are the energy fractions for  $Q$  and  $\bar{Q}'$  in the meson, respectively. The explicit expressions for all the momentum in the rest frame of the  $B_c$  meson are given by

$$P_{B_c}^\mu = (E_1 + E_2, 0), \quad (23)$$

$$q^\mu = (0, \mathbf{q}), \quad (24)$$

$$p_1^\mu = (E_1, -\mathbf{q}), \quad (25)$$

$$p_2^\mu = (E_2, \mathbf{q}). \quad (26)$$

In the rest frame, the meson momentum becomes purely time-like while the relative momentum is spacelike. One obtains the relations  $\alpha = \sqrt{m_b^2 - q^2}/(\sqrt{m_b^2 - q^2} + \sqrt{m_c^2 - q^2})$  and  $\beta = 1 - \alpha$  with the on-shell conditions  $E_1 = \sqrt{m_b^2 - q^2}$ ,  $E_2 = \sqrt{m_c^2 - q^2}$ , and  $q^2 = -\mathbf{q}^2$ .

#### 3.2 Covariant projection method

In the following calculation, we will adopt the covariant spin-projector method, which can be applied to all orders in  $v$ .

The Dirac spinors for the  $B_c$  system may be written as

$$u_b(p_1, \lambda) = \sqrt{\frac{E_1 + m_b}{2E_1}} \begin{pmatrix} \xi_\lambda \\ \frac{\vec{\sigma} \cdot \vec{p}_1}{E_1 + m_b} \xi_\lambda \end{pmatrix}, \quad (27)$$

$$v_c(p_2, \lambda) = \sqrt{\frac{E_2 + m_c}{2E_2}} \begin{pmatrix} \frac{\vec{\sigma} \cdot \vec{p}_2}{E_2 + m_c} \xi_\lambda \\ \xi_\lambda \end{pmatrix}, \quad (28)$$

where  $\xi_\lambda$  is the two-component Pauli spinors and  $\lambda$  is the polarization parameters. It is straightforward to derive the covariant form of the spin-singlet combinations of the spinor bilinears:

$$\begin{aligned} \Pi_0(q) &= -i \sum_{\lambda_1, \lambda_2} u_b(p_1, \lambda_1) \bar{v}_c(p_2, \lambda_2) \left\langle \frac{1}{2} \lambda_1 \frac{1}{2} \lambda_2 | 00 \right\rangle \\ &\quad \otimes \frac{1_c}{\sqrt{N_c}} \\ &= \frac{i}{4\sqrt{2}E_1E_2\omega} (\alpha \not{P}_{B_c} - \not{q} + m_b) \frac{\not{P}_{B_c} + E_1 + E_2}{E_1 + E_2} \gamma_5 \\ &\quad \times (\beta \not{P}_{B_c} + \not{q} - m_c) \otimes \frac{1_c}{\sqrt{N_c}}, \end{aligned} \quad (29)$$

with the auxiliary parameter  $\omega = \sqrt{E_1 + m_b} \sqrt{E_2 + m_c}$ . Here  $1_c$  is the unit matrix in the fundamental representation of the color SU(3) group.

#### 3.3 Perturbative matching

Due to the simplicity of the final state, one can directly match the QCD currents onto the NRQCD ones. To determine the values of  $c_0$  and  $c_2$ , we work in the spirit of taking those short-distance coefficients to be insensitive to the long-distance hadronic dynamics. As a convenient choice, one can replace the physical  $B_c^-$  meson by a free  $\bar{c}b$  pair of the quantum number  $^1S_0^{[1]}$ , so that both the full amplitude,  $\mathcal{A}[\bar{c}b(^1S_0^{[1]}) \rightarrow \gamma \ell \bar{\nu}]$ , and the NRQCD operator matrix elements can be directly accessed in perturbation theory. The short-distance coefficients  $c_i$  can then be solved by equating the QCD amplitude  $\mathcal{A}$  and the corresponding NRQCD amplitude, order by order in  $\alpha_s$ . For this purpose, we introduce a decay constant and two form factors at the free quark level:

$$\langle 0 | \bar{c} \gamma_\mu \gamma_5 b | \bar{c} b(^1S_0^{[1]}) \rangle = i \bar{U} g_{\mu 0}, \quad (30)$$

$$\langle \gamma(\epsilon, k) | \bar{c} \gamma_\mu b | \bar{c} b(^1S_0^{[1]}) \rangle = -e \frac{1}{k \cdot P_{B_c}} \mathbb{V} \epsilon_{\mu\nu\rho\sigma} \epsilon^{*\nu} P_{B_c}^\rho k^\sigma, \quad (31)$$

$$\begin{aligned} \langle \gamma(\epsilon, k) | \bar{c} \gamma_\mu \gamma_5 b | \bar{c} b(^1S_0^{[1]}) \rangle &= i e \mathbb{A} \left( \epsilon_\mu^* - k_\mu \frac{P_{B_c} \cdot \epsilon^*}{P_{B_c} \cdot k} \right) \\ &\quad - i e \frac{1}{P_{B_c} \cdot k} \bar{U} P_{B_c \mu} P_{B_c} \cdot \epsilon^*. \end{aligned} \quad (32)$$

<sup>2</sup> Throughout this paper, we shall use the superscripts (0) and (1) to indicate the LO and NLO contributions in  $\alpha_s$  and the subscripts 0 and 2 to denote the LO and NLO contributions in the velocity.

Analogous to (18–20), one can write down the matching formula:

$$\mathcal{U} = c_0^f \langle 0 | \chi_c^\dagger \psi_b | \bar{c}b(^1S_0^{[1]}) \rangle + \frac{c_2^f}{(m_b + m_c)^2} \times \left\langle 0 \left| \chi_c^\dagger \left( -\frac{i}{2} \overleftrightarrow{\mathbf{D}} \right)^2 \psi_b \right| \bar{c}b(^1S_0^{[1]}) \right\rangle, \quad (33)$$

$$\mathcal{V} = \frac{1}{m_b + m_c} \left[ c_0^V \langle 0 | \chi_c^\dagger \psi_b | \bar{c}b(^1S_0^{[1]}) \rangle + \frac{c_2^V}{(m_b + m_c)^2} \times \left\langle 0 \left| \chi_c^\dagger \left( -\frac{i}{2} \overleftrightarrow{\mathbf{D}} \right)^2 \psi_b \right| \bar{c}b(^1S_0^{[1]}) \right\rangle \right], \quad (34)$$

$$\mathcal{A} = \frac{1}{m_b + m_c} \left[ c_0^A \langle 0 | \chi_c^\dagger \psi_b | \bar{c}b(^1S_0^{[1]}) \rangle + \frac{c_2^A}{(m_b + m_c)^2} \times \left\langle 0 \left| \chi_c^\dagger \left( -\frac{i}{2} \overleftrightarrow{\mathbf{D}} \right)^2 \psi_b \right| \bar{c}b(^1S_0^{[1]}) \right\rangle \right], \quad (35)$$

where we have adopted the nonrelativistic normalization.

One can organize the full amplitudes defined in Eqs. (30)–(32) in powers of the relative momentum between  $\bar{c}$  and  $b$ , denoted by  $\mathbf{q}$ . To the desired accuracy, one can truncate the series at  $\mathcal{O}(\mathbf{q}^2)$ , with the first two Taylor coefficients. We will compute both amplitudes at LO in  $\alpha_s$  in Sect. 3.4, and the calculation at NLO in  $\alpha_s$  will be conducted in Sect. 3.5.

The NRQCD matrix elements encountered in the above equations are particularly simple at LO in  $\alpha_s$ :

$$\langle 0 | \chi^\dagger \psi | \bar{c}b(^1S_0^{[1]}) \rangle^{(0)} = \sqrt{2N_c},$$

$$\left\langle 0 \left| \chi^\dagger \left( -\frac{i}{2} \overleftrightarrow{\mathbf{D}} \right)^2 \psi \right| \bar{c}b(^1S_0^{[1]}) \right\rangle^{(0)} = \sqrt{2N_c} \mathbf{q}^2, \quad (36)$$

where the factor  $\sqrt{2N_c}$  is due to the spin and color factors of the normalized  $\bar{c}b(^1S_0^{[1]})$  state. The computation of these matrix elements to  $\mathcal{O}(\alpha_s)$  will be addressed in Sect. 3.6.

### 3.4 Tree-level amplitude

Adopting the above notation, one can easily obtain the tree-level amplitude for the decay constant,

$$\begin{aligned} \langle 0 | \bar{c} \gamma_\mu \gamma_5 b | \bar{c}b(^1S_0^{[1]}) \rangle^{(0)} &= \text{Tr} [\Pi_0(q) \gamma_\mu \gamma_5] \\ &= i p_{B_c}^\mu \sqrt{2N_c} \frac{(E_1 + m_b)(E_2 + m_c) + q^2}{2\sqrt{E_1 E_2 (E_1 + m_b)(E_2 + m_c)}(E_1 + E_2)} \\ &= i g_{\mu 0} \sqrt{2N_c} \left( 1 - \frac{q^2}{8m_{\text{red}}^2} \right), \end{aligned} \quad (37)$$

where the  $q^\mu$  terms have been omitted and

$$m_{\text{red}} = \frac{m_b m_c}{m_b + m_c} \quad (38)$$

is defined as the reduced mass of the  $\bar{c}b$  system.

The vector current is similarly evaluated as

$$\begin{aligned} &\langle \gamma | \bar{c} \gamma_\mu b | \bar{c}b(^1S_0^{[1]}) \rangle^{(0)} \\ &= \text{Tr} \left[ \Pi_0(q) i e e_c \not{\epsilon}^* \frac{i(\not{k} - \not{p}_2 + m_c)}{(k - p_2)^2 - m_c^2} \gamma_\mu \right] \\ &\quad + \text{Tr} \left[ \Pi_0(q) \gamma_\mu \frac{i(\not{p}_1 - \not{k} + m_b)}{(p_1 - k)^2 - m_b^2} i e e_b \not{\epsilon}^* \right] \\ &= -\frac{e\sqrt{2N_c}}{4w\sqrt{E_1 E_2}} \left( \frac{e_c}{E_2 k \cdot p_{B_c} + E k \cdot q} \right. \\ &\quad \left. + \frac{e_b}{E_1 k \cdot p_{B_c} - E k \cdot q} \right) \\ &\quad \times \{ E_{bc} \epsilon_{\mu\nu\rho\sigma} \epsilon^{*\nu} k^\rho p_{B_c}^\sigma + E(E_1 + E_2 + m_b - m_c) \\ &\quad \times \epsilon_{\mu\nu\rho\sigma} \epsilon^{*\nu} k^\rho q^\sigma \}. \end{aligned} \quad (39)$$

We have introduced the abbreviations  $E = E_1 + E_2$  and  $E_{bc} = (E_1 + m_b)(E_2 + m_c) + q^2$ . Here  $e_c = 2/3$  and  $e_b = -1/3$  are the electric charges of the  $c$  and  $b$  quark, respectively.

One can perform the Taylor expansion of the amplitudes in powers of  $q^\mu$ :

$$\mathcal{A}(q) = \mathcal{A}(0) + \frac{\partial \mathcal{A}(0)}{\partial q^\mu} \bigg|_{q=0} q^\mu + \frac{1}{2!} \frac{\partial^2 \mathcal{A}(0)}{\partial q^\mu \partial q^\nu} \bigg|_{q=0} q^\mu q^\nu + \dots \quad (40)$$

Those terms linear in  $q$  should be dropped, since they do not contribute to the short-distance coefficient. In this paper, the  $\mathcal{O}(|\mathbf{q}|^2)$  contributions will be retained. In order to simplify the calculation in the covariant derivation, one should use the following replacement:

$$q^\mu q^\nu \rightarrow \frac{|\mathbf{q}|^2}{D-1} \left( -g^{\mu\nu} + \frac{P_{B_c}^\mu P_{B_c}^\nu}{P_{B_c}^2} \right). \quad (41)$$

The result for the axial-vector current is a bit lengthy:

$$\begin{aligned} &\langle \gamma | \bar{c} \gamma_\mu \gamma_5 b | \bar{c}b(^1S_0^{[1]}) \rangle^{(0)} \\ &= -i e \sqrt{2N_c} \frac{1}{4\sqrt{E_1 E_2 (E_1 + m_b)(E_2 + m_c)}} \\ &\quad \times \left\{ \epsilon_\mu^* e_c \frac{k \cdot p_{B_c} E_{bc} + k \cdot q E (E_1 - E_2 + m_b - m_c)}{E_2 k \cdot p_{B_c} + E k \cdot q} \right. \\ &\quad - \epsilon_\mu^* e_b \frac{k \cdot p_{B_c} E_{bc} + k \cdot q E (E_1 - E_2 + m_b - m_c)}{E_1 k \cdot p_{B_c} - E k \cdot q} \\ &\quad + q_\mu e_c \frac{2(E_1 - E_2 + m_b - m_c)(E_2 \epsilon^* \cdot p_{B_c} + E \epsilon^* \cdot q)}{E_2 k \cdot p_{B_c} + E k \cdot q} \\ &\quad - q_\mu e_b \frac{2(E_1 - E_2 + m_b - m_c)(E_1 \epsilon^* \cdot p_{B_c} - E \epsilon^* \cdot q)}{E_1 k \cdot p_{B_c} - E k \cdot q} \\ &\quad + p_{B_c \mu} e_c \frac{2E_{bc}(E_2 \epsilon^* \cdot p_{B_c} + E \epsilon^* \cdot q)}{E(E_2 k \cdot p_{B_c} + E k \cdot q)} \\ &\quad \left. - p_{B_c \mu} e_b \frac{2(E_1 E_{bc} \epsilon^* \cdot p_{B_c} + E \epsilon^* \cdot q(E_{bc} + q^2))}{E(E_1 k \cdot p_{B_c} - E k \cdot q)} \right\} \end{aligned}$$

$$\begin{aligned} & -k_\mu e_c \frac{E_{bc} \epsilon^* \cdot p_{B_c} + E \epsilon^* \cdot q (E_1 - E_2 + m_b - m_c)}{E_2 k \cdot p_{B_c} + E k \cdot q} \\ & + k_\mu e_b \frac{E_{bc} \epsilon^* \cdot p_{B_c} + E \epsilon^* \cdot q (E_1 - E_2 + m_b - m_c)}{E_1 k \cdot p_{B_c} - E k \cdot q} \Big\}. \end{aligned} \quad (42)$$

In order to extract the  $\mathcal{A}$  form factor, we only need to keep the  $\epsilon_\mu$  term which corresponds to Feynman gauge  $\epsilon \cdot p_{B_c} = 0$ , but we have explicitly checked the gauge invariance up to  $v^2$  order.

The tree-level NRQCD matrix elements for  $\bar{c}b$  are given in Eq. (36), and thus the above results in Eqs. (37), (39), and (42) lead to the tree-level Wilson coefficients,

$$c_0^{f,0} = 1, \quad (43)$$

$$c_2^{f,0} = -\frac{\tilde{z}^4}{8z^2}, \quad (44)$$

$$c_0^{V,0} = -\frac{e_c}{2z} - \frac{e_b}{2}, \quad (45)$$

$$c_2^{V,0} = -\tilde{z}^2 \left( \frac{e_c(3z^2 + 2z + 11)}{48z^3} + \frac{e_b(11z^2 + 2z + 3)}{48z^2} \right), \quad (46)$$

$$c_0^{A,0} = \frac{e_b}{2} - \frac{e_c}{2z}, \quad (47)$$

$$c_2^{A,0} = -\tilde{z}^2 \left( \frac{e_c[(3z^2 + 2z + 11) + 8z(1-z)m_b/E_k]}{48z^3} - \frac{e_b[(11z^2 + 2z + 3) - 8z(1-z)m_b/E_k]}{48z^2} \right). \quad (48)$$

In the above results, we have defined  $z = m_c/m_b$  and  $\tilde{z} = 1 + z$ .  $c_i^{f,0}$  means the LO of the Wilson coefficient  $c_i^f$ . It is interesting to notice that the Wilson coefficient  $c_2^{A,0}$  depends on the energy of the emitted photon, which will induce a nontrivial behavior, as will be demonstrated later.

### 3.5 NLO amplitudes in QCD

Typical one-loop diagrams for the QCD corrections to the  $B_c \rightarrow \gamma \ell \bar{\nu}_\ell$  decay are shown in Fig. 2. In calculating the one-loop amplitudes, we use the dimensional regularization to regulate the ultraviolet (UV) and infrared (IR) divergence.

The diagram (a) in Fig. 2 contributes to the NLO decay constant:

$$\begin{aligned} \mathcal{U}_{0,a}^1 &= \sqrt{2N_c} \frac{C_F \alpha_s}{4\pi} \left[ \frac{1}{\hat{\epsilon}_{UV}} + \frac{2}{\hat{\epsilon}_{IR}} + 3 \ln \frac{\mu^2}{m_b^2} - 2 \right. \\ & \quad \left. + 2t_1 - \frac{6 \ln z}{z+1} \right], \end{aligned} \quad (49)$$

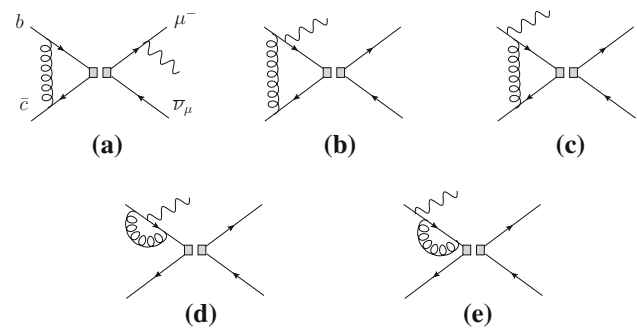


**Fig. 2** Typical NLO Feynman diagrams for the radiative leptonic  $B_c \rightarrow \gamma \mu \bar{\nu}_\mu$  decay in the SM. The other four diagrams can easily be obtained by interchanging the bottom and anti-charm quarks lines

with

$$t_1 = \frac{1}{2|v|} \left( \pi^2 - i\pi \left[ \frac{1}{\hat{\epsilon}_{IR}} - \ln \frac{16m_{red}^2 |v|^2}{\mu^2} \right] \right), \quad (50)$$

We have introduced the abbreviation

$$\frac{1}{\hat{\epsilon}_{UV,IR}} = \frac{1}{\epsilon_{UV,IR}} - \gamma_E + \ln 4\pi. \quad (51)$$

The heavy quark field renormalization and mass term are given as

$$\begin{aligned} Z_q^{OS} &= 1 - \frac{C_F \alpha_s}{4\pi} \left[ \frac{1}{\hat{\epsilon}_{UV}} + \frac{2}{\hat{\epsilon}_{IR}} + 3 \ln \frac{\mu^2}{m^2} + 4 \right], \\ \delta_m &= -\frac{3m C_F \alpha_s}{4\pi} \left[ \frac{1}{\hat{\epsilon}_{UV}} + \ln \frac{\mu^2}{m^2} + \frac{4}{3} \right]. \end{aligned} \quad (52)$$

For the vector current form factor, the sub-diagram in Fig. 2 gives out the corresponding contribution

$$\begin{aligned} \mathbb{V}_b &= \frac{\sqrt{2N_c} e_b C_F \alpha_s}{4\pi m_b} \left[ -\frac{1}{\hat{\epsilon}_{IR}} + \frac{4\tilde{z}}{y^2 - \tilde{z}^2} + \frac{\tilde{z}^2 + y^2}{y^2 \tilde{z} - \tilde{z}^3} b_1 \right. \\ & \quad \left. - \frac{1}{\tilde{z}} b_2 + \frac{2(y^2 - z(z+1))}{z(y^2 - \tilde{z}^2)} b_3 - \frac{2y^2}{z(y^2 - \tilde{z}^2)} b_4 \right. \\ & \quad \left. - \frac{y^2}{\tilde{z}} c_4 - (1-z)c_3 - (\tilde{z}^2 - y^2)d_1 \right], \\ \mathbb{V}_c &= \frac{\sqrt{2N_c} e_b C_F \alpha_s}{4\pi m_b} \left[ -\frac{1}{2} \frac{1}{\hat{\epsilon}_{UV}} + \frac{y^2 + z^2 + 4z + 3}{\tilde{z}^2 - y^2} \right. \\ & \quad \left. + \frac{\tilde{z} + y^2}{\tilde{z}^2 - y^2} b_1 - \frac{\tilde{z}(3y^2 - z^2 + 1)}{2z(\tilde{z}^2 - y^2)} b_4 \right. \\ & \quad \left. + \frac{(2z^2 + 3z - 1)\tilde{z} - y^2(2z + 3)}{2z(y^2 - \tilde{z}^2)} b_3 \right. \\ & \quad \left. + (\tilde{z} + y^2 - z^2)c_4 \right], \\ \mathbb{V}_d &= \frac{\sqrt{2N_c} e_b C_F \alpha_s}{4\pi m_b} \left[ -\frac{1}{2} \frac{1}{\hat{\epsilon}_{UV}} + \frac{y^2 - z^2 + 4z + 5}{\tilde{z}^2 - y^2} \right. \end{aligned}$$



$$\begin{aligned} & + \frac{y^2 - z^2 + z + 2}{\tilde{z}^2 - y^2} b_2 + \frac{y^2 - z^2 + 4z + 5}{2(y^2 - \tilde{z}^2)} b_3 + c_1 \Big], \\ \mathbb{V}_e = & \frac{\sqrt{2N_c} e_b C_F \alpha_s}{4\pi m_b} \left[ \frac{-y^2 + z^2 + 8z + 7}{2(\tilde{z}^2 - y^2)} + \frac{\tilde{z}^2 - y^2}{2(y^2 - z\tilde{z})} \right. \\ & - \frac{\tilde{z}(y^2 - z^2 + 1)}{2(y^2 - z\tilde{z})(y^2 - \tilde{z}^2)} b_2 \\ & \left. + \frac{(z^2 + 6z + 1)\tilde{z}^2 + y^4 - 2y^2(z^2 + 4z + 3)}{2(y^2 - \tilde{z}^2)(y^2 - z\tilde{z})} b_3 \right], \end{aligned} \quad (53)$$

where the auxiliary functions  $b_i$ ,  $c_i$ , and  $d_i$  are defined in Appendix B.

The mass counter-terms and wave function renormalization corrections give

$$\begin{aligned} \mathbb{V}_{\text{CT}-m} &= \frac{\sqrt{2N_c} e_b C_F \alpha_s}{4\pi m_b} \left[ \frac{3\tilde{z}}{y^2 - \tilde{z}^2} \left( \frac{1}{\hat{\epsilon}_{\text{UV}}} + \ln \frac{\mu^2}{m_b^2} + \frac{4}{3} \right) \right], \\ \mathbb{V}_{\text{CT}-F} &= \frac{\sqrt{2N_c} e_b C_F \alpha_s}{4\pi m_b} \left[ \frac{1}{\hat{\epsilon}_{\text{IR}}} + \frac{1}{2} \frac{1}{\hat{\epsilon}_{\text{UV}}} + \frac{3}{2} \ln \frac{\mu^2}{zm_b^2} + 2 \right]. \end{aligned} \quad (54)$$

For the axial-vector current form factor, the sub-diagram has gauge-dependent contributions; however, the summed result is gauge invariant. We will show the details in Appendix C.

### 3.6 NLO amplitudes in NRQCD

The NRQCD Lagrangian can be derived by integrating out the degrees of freedom of order heavy quark mass [53]:

$$\begin{aligned} \mathcal{L}_{\text{NRQCD}} = & \psi^\dagger \left( iD_t + \frac{\mathbf{D}^2}{2m} \right) \psi + \psi^\dagger \frac{\mathbf{D}^4}{8m^3} \psi \\ & + \frac{c_F}{2m} \psi^\dagger \boldsymbol{\sigma} \cdot g_s \mathbf{B} \psi + \frac{c_D}{8m^2} \psi^\dagger \\ & \times (\mathbf{D} \cdot g_s \mathbf{E} - g_s \mathbf{E} \cdot \mathbf{D}) \psi \\ & + \frac{ic_S}{8m^2} \psi^\dagger \boldsymbol{\sigma} \cdot (\mathbf{D} \times g_s \mathbf{E} - g_s \mathbf{E} \times \mathbf{D}) \psi \\ & + \left( \psi \rightarrow i\sigma^2 \chi^*, A_\mu \rightarrow -A_\mu^T \right) + \mathcal{L}_{\text{light}}. \end{aligned} \quad (55)$$

The replacement in the last line implies that the corresponding heavy anti-quark bilinear sector can be obtained through the charge conjugation transformation.  $\mathcal{L}_{\text{light}}$  represents the Lagrangian for the light quarks and gluons. The coefficients  $c_D$ ,  $c_F$ , and  $c_S$  have perturbative expansions in powers of  $\alpha_s$ , which can be written as  $c_i = 1 + \mathcal{O}(\alpha_s)$ .

The matrix element of the  $\bar{c}b$  to vacuum at NLO can be written as

$$\begin{aligned} & \langle 0 | \chi^\dagger \psi | \bar{c}b(^1S_0^{[1]}) \rangle^{(1)} \\ &= \sqrt{2N_c} \frac{\alpha_s C_F}{2\pi} \frac{1}{2|v|} \left( \pi^2 - i\pi \left[ \frac{1}{\epsilon_{\text{IR}}} - \ln \frac{16m_{\text{red}}^2 |v|^2}{\mu^2} \right] \right). \end{aligned} \quad (56)$$

This is in agreement with the results in Ref. [71].

### 3.7 Determination of $c_i$ : matching QCD to NRQCD

Up to  $\alpha_s$  and  $v^2$ , one can expand the decay constant and form factors as

$$\begin{aligned} \mathbb{U} = & c_0^{f,0} \langle 0 | \chi_c^\dagger \psi_b | \bar{c}b(^1S_0^{[1]}) \rangle^{(0)} + c_0^{f,1} \langle 0 | \chi_c^\dagger \psi_b | \bar{c}b(^1S_0^{[1]}) \rangle^{(0)} \\ & + c_0^{f,0} \langle 0 | \chi_c^\dagger \psi_b | \bar{c}b(^1S_0^{[1]}) \rangle^{(1)} \\ & + \frac{c_2^{f,0}}{(m_b + m_c)^2} \left\langle 0 \left| \chi_c^\dagger \left( -\frac{i}{2} \overleftrightarrow{D} \right)^2 \psi_b \right| \bar{c}b(^1S_0^{[1]}) \right\rangle^{(0)}, \end{aligned} \quad (57)$$

$$\begin{aligned} \mathbb{V} = & \frac{1}{m_b + m_c} \left[ c_0^{V,0} \langle 0 | \chi_c^\dagger \psi_b | \bar{c}b(^1S_0^{[1]}) \rangle^{(0)} \right. \\ & + c_0^{V,1} \langle 0 | \chi_c^\dagger \psi_b | \bar{c}b(^1S_0^{[1]}) \rangle^{(0)} + c_0^{V,0} \langle 0 | \chi_c^\dagger \psi_b | \bar{c}b(^1S_0^{[1]}) \rangle^{(1)} \\ & \left. + \frac{c_2^{V,0}}{(m_b + m_c)^2} \left\langle 0 \left| \chi_c^\dagger \left( -\frac{i}{2} \overleftrightarrow{D} \right)^2 \psi_b \right| \bar{c}b(^1S_0^{[1]}) \right\rangle^{(0)} \right], \end{aligned} \quad (58)$$

$$\begin{aligned} \mathbb{A} = & \frac{1}{m_b + m_c} \left[ c_0^{A,0} \langle 0 | \chi_c^\dagger \psi_b^{(0)} | \bar{c}b(^1S_0^{[1]}) \rangle^{(0)} \right. \\ & + c_0^{A,1} \langle 0 | \chi_c^\dagger \psi_b^{(0)} | \bar{c}b(^1S_0^{[1]}) \rangle^{(0)} \\ & + c_0^{A,0} \langle 0 | \chi_c^\dagger \psi_b^{(0)} | \bar{c}b(^1S_0^{[1]}) \rangle^{(1)} \\ & \left. + \frac{c_2^{A,0}}{(m_b + m_c)^2} \left\langle 0 \left| \chi_c^\dagger \left( -\frac{i}{2} \overleftrightarrow{D} \right)^2 \psi_b \right| \bar{c}b(^1S_0^{[1]}) \right\rangle^{(0)} \right]. \end{aligned} \quad (59)$$

Matching the QCD results onto the NRQCD, one can obtain the UV and IR finite short-distance coefficient,

$$\begin{aligned} c_0^{f,1} &= -\frac{3C_F \alpha_s}{4\pi} \left( 2 + \frac{1-z}{1+z} \ln z \right), \\ c_0^{V,1} &= \frac{C_F \alpha_s}{4\pi} \left\{ e_b \left[ \ln \frac{\mu^2}{zm_b^2} - \frac{\tilde{z}^2(-3z\tilde{z} + \tilde{z} + 2y^2) + y^4}{2(y^2 - z\tilde{z})(y^2 - \tilde{z}^2)} \right. \right. \\ & + \frac{\tilde{z}^3 + y^2(3z - 1)}{4(\tilde{z}^3 - y^2\tilde{z})} b_1 + \frac{y^2 - 2z\tilde{z}}{2z(y^2 - z\tilde{z})} b_3 \\ & + \frac{1}{4} \left( \frac{2\tilde{z}}{y^2 - z\tilde{z}} + \frac{2}{\tilde{z} - y} + \frac{2}{\tilde{z} + y} - \frac{4}{\tilde{z}} - 3 \right) b_2 \\ & + \frac{-z\tilde{z}^2 + \tilde{z}^2 + 3y^2z - y^2}{2z(y^2 - \tilde{z}^2)} b_4 \\ & \left. + \frac{-\tilde{z} - y^2z + z^3 + z^2}{z\tilde{z}} c_1 + \frac{y^2z - z^3 + 2z + 1}{z} c_2 \right\} \end{aligned} \quad (60)$$

$$+ (z-1)c_3 + (y^2 - \tilde{z}^2)d_1 \Bigg] + \left( e_b \rightarrow \frac{e_c}{z}, z \rightarrow \frac{1}{z}, y \rightarrow \frac{y}{z} \right) \Bigg\}, \quad (61)$$

$$\begin{aligned} c_0^{A,1} = & \frac{C_F \alpha_s}{4\pi} \left\{ e_b \left[ -\ln \frac{\mu^2}{zm_b^2} + \frac{1}{2(y^2 - z\tilde{z})(y^2 - \tilde{z}^2)^2} \right. \right. \\ & \times (y^4(z+1)\tilde{z} - y^2(z(5z+34) + 5)\tilde{z}^2 \\ & + (z(z(3z+23) + 5) + 1)\tilde{z}^3 + y^6) + \frac{b_1}{4\tilde{z}(y^2 - \tilde{z}^2)^2} \\ & \times (-2y^2(z-3)\tilde{z}^2 - (z^2 + 14z - 3)\tilde{z}^3 + y^4(3z-1)) \\ & + \frac{b_2}{4\tilde{z}(y^2 - z\tilde{z})(y^2 - \tilde{z}^2)} (y^2(y^2(3z+7) \\ & - (2z+3)(3z-1)\tilde{z}) + (3(z-1)z-2)\tilde{z}^3) \\ & - \frac{b_3}{2z(z\tilde{z} - y^2)(y^2 - \tilde{z}^2)^2} (y^2(13z^2 - 2z + 1)\tilde{z}^2 \\ & - 2(3z^3 + z)\tilde{z}^3 + y^4(y^2 - 8z^2 - 6z + 2)) \\ & - \frac{(z-1)^2\tilde{z}^3 + y^4(3z+1) - 2y^2(2z^3 + 5z^2 + 2z - 1)}{2z(y^2 - \tilde{z}^2)^2} b_4 \\ & + \frac{y^2(y^2(-z) + z^2(2z+5) - 3) - (z-1)(z(z+4) - 1)\tilde{z}^2}{z\tilde{z}(\tilde{z}^2 - y^2)} c_1 \\ & - \frac{((z-2)z(z+4) + 1)\tilde{z}^2 + y^2(z(y^2 - 2z(z+2) + 3) + 3)}{z(y - \tilde{z})(\tilde{z} + y)} c_2 \\ & + \frac{(z-1)(-y^2 + z^2 - 1)}{y^2 - \tilde{z}^2} c_3 + (-y^2 + z^2 + 4z - 1)d_1 \Bigg] \\ & \left. - \left( e_b \rightarrow \frac{e_c}{z}, z \rightarrow \frac{1}{z}, y \rightarrow \frac{y}{z} \right) \right\}. \quad (62) \end{aligned}$$

Note that the scale-dependent terms in the braces of Eqs. (61) and (62) will cancel each other; the residual dependence only lies in the strong coupling constant. The result for the short-distance coefficient  $c_0^{f,1}$  is in agreement with the previous calculation in Ref. [72].

#### 4 Phenomenological results

The input parameters are adopted as [73]:  $m_{B_c} = 6.2756 \text{ GeV}$ ;  $G_F = 1.16637 \times 10^{-5} \text{ GeV}^{-2}$ ;  $\alpha = 1/128$ ; for the CKM parameters, we adopt  $|V_{cb}| = 0.041$ . For the heavy quark mass, we adopt  $m_b = 4.8 \text{ GeV}$  and  $m_c = 1.5 \text{ GeV}$  [46]. The  $B_c$ -meson lifetime is taken using the latest measurement by the LHCb Collaboration, i.e.  $\tau_{B_c} = 0.50 \text{ ps}$  [5, 6].

We first present the numerical results for the decay constant  $f_{B_c}$ :

$$\begin{aligned} 1.07c_2^{f,0} &= -\frac{\tilde{z}^4}{8\tilde{z}^2} = -3.8, \\ c_0^{f,1} &= -\frac{3C_F\alpha_s}{4\pi} \left( 2 + \frac{1-z}{1+z} \ln z \right) = -0.44 \times \alpha_s. \end{aligned} \quad (63)$$

The strong coupling constant at the Z-boson peak is [73]

$$\alpha_s(m_Z) = 0.1185 \pm 0.0006, \quad (64)$$

which corresponds to

$$\alpha_s(m_b) = 0.218, \quad \alpha_s(m_c) = 0.368. \quad (65)$$

With these values, one can see that the  $\alpha_s$  corrections can reduce the decay constant by approximately 9.5–16.2 %.

To estimate the size of  $\mathcal{O}(|\mathbf{v}|^2)$  effects, one requires the size of non-perturbative LDMEs, for which we use a Buchmüller–Tye (B-T) potential model [74]:

$$\langle 0 | \chi_c^\dagger \psi_b | \overline{B}_c(\mathbf{p}) \rangle = x \sqrt{\frac{N_c}{2\pi}} |R_S^{B-T}(0)| \simeq 0.884 \text{ GeV}^{3/2}, \quad (66)$$

$$\left\langle 0 \left| \chi_c^\dagger \left( -\frac{i}{2} \overleftrightarrow{\mathbf{D}} \right)^2 \psi_b \right| \overline{B}_c(\mathbf{p}) \right\rangle \simeq \mathbf{q}^2 \langle 0 | \chi_c^\dagger \psi_b | \overline{B}_c(\mathbf{p}) \rangle. \quad (67)$$

For an estimate of  $\mathbf{q}^2$ , one may make use of the relative velocity. Using the heavy quarks kinetic and potential energy approximation [53], we have

$$|\mathbf{v}| \simeq \alpha_s(2m_{\text{red}}|\mathbf{v}|). \quad (68)$$

Choosing  $m_b = 4.8 \text{ GeV}$  and  $m_c = 1.5 \text{ GeV}$ , and using the two-loop strong coupling constant, we get

$$|\mathbf{v}|_{J/\psi}^2 \simeq 0.267, \quad |\mathbf{v}|_{\Upsilon}^2 \simeq 0.108, \quad |\mathbf{v}|_{B_c}^2 \simeq 0.186. \quad (69)$$

For a value  $\langle \mathbf{v}^2 \rangle_{B_c} \simeq 0.186$ , we have

$$\mathbf{q}^2 \simeq 0.9718 \text{ GeV}^2. \quad (70)$$

As a result, the decay constant will be further reduced by about 9 %.

For the short-distance coefficients for the  $B_c \rightarrow \gamma$  transition form factors  $V$  and  $A$ , our results are shown in Fig. 3. The solid line denotes the leading-order coefficient  $c_0^{V(A),0}$ , the dotted line correspond to the coefficient  $c_2^{V(A),0}$  from relativistic corrections, and the thick curve is the coefficient  $c_0^{V(A),2}$  from  $\alpha_s$  corrections. From these figures, one can see that the relativistic corrections give constructive contributions, but the  $\mathcal{O}(\alpha_s)$  QCD corrections are destructive and thus have important consequences.

With the estimated long-distance matrix elements, the results for differential distributions are given in Figs. 4 and 5, where the QCD and relativistic corrections are shown, respectively. The integrated branching ratios of  $B_c \rightarrow \gamma \ell \bar{\nu}$  and  $B_c \rightarrow \ell \bar{\nu}$  are presented in Tables 1, 2, and 3. Note that the factorization in Eqs. (18)–(20) is valid only for a hard photon, while the soft-photon contribution requires special treatment [70]. Thus a cut-off on the photon energy should be introduced, and we adopt three cases for the estimate of errors, i.e.  $E_k \geq 0.25 \text{ GeV}$  for Cut-I,  $E_k \geq 0.5 \text{ GeV}$  for Cut-II, and  $E_k \geq 1 \text{ GeV}$  for Cut-III, where the corresponding results



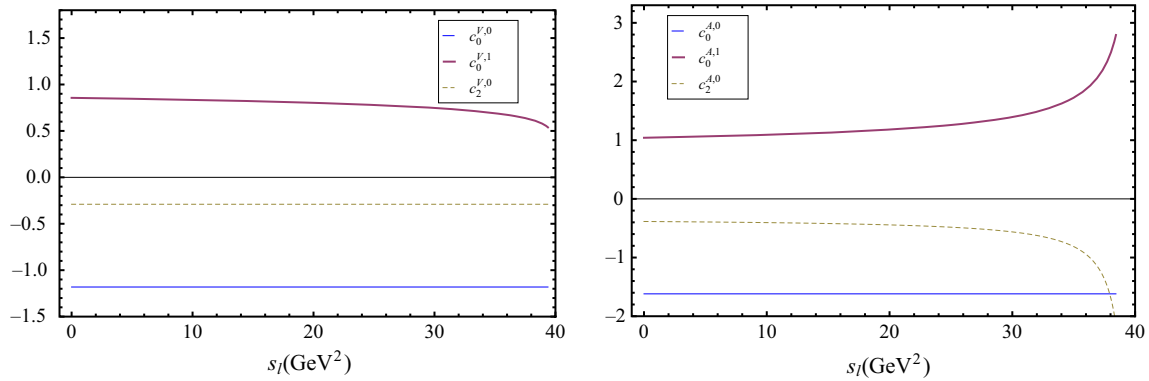


**Fig. 3** Dependence of short-distance coefficients  $c^{V(A)}$  on the  $s_l$ . The solid line denotes the coefficient  $c_0^{V(A),0}$ , the dotted line is the coefficient  $c_2^{V(A),0}$  from relativistic corrections, and the thick

curve is the coefficient  $c_0^{V(A),2}$  from  $\alpha_s$  corrections. The results are not valid for a soft photon, which corresponds to  $s_l \sim m_{B_c}^2$

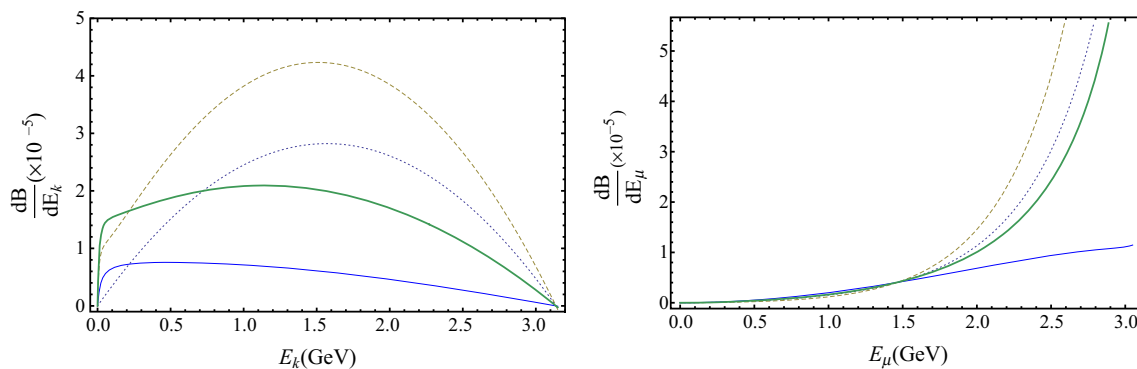


**Fig. 4** The dependence of the branching ratio  $\mathcal{B}(B_c \rightarrow \gamma \mu \bar{\nu}_\mu)$  on the photon and lepton energy. The dotted line denotes the leading-order result, the dashed line is the result with relativistic corrections, the blue line is the result with QCD corrections, and the thick curve denotes

the total results with both the QCD and the relativistic corrections. The results are not valid for a soft photon, namely when  $E_k$  becomes small, and  $E_l$  becomes large

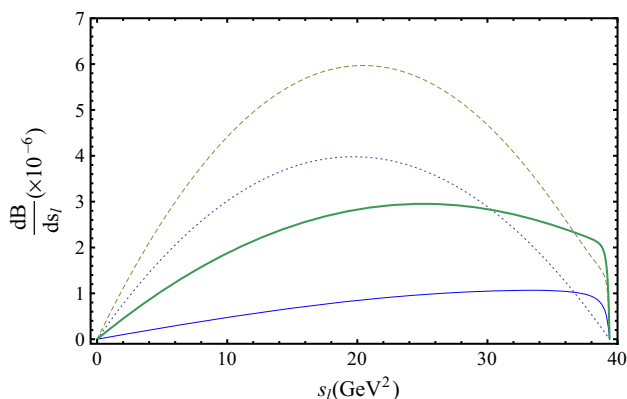


**Fig. 5** Similar to Fig. 4 but for the  $s_l$  dependence. The results are not valid for a soft photon, which corresponds to the region where  $s_l \sim m_{B_c}^2$

are given in Table 2. Ignoring the lepton mass, the branching ratio of  $B_c \rightarrow \gamma e \bar{\nu}_e$  is identical to that of  $B_c \rightarrow \gamma \mu \bar{\nu}_\mu$ . The LO results are in agreement with Refs. [54–58] with the same input parameters. From the calculation, one can see that both the QCD and the relativistic corrections give

destructive contributions to the process  $B_c \rightarrow \ell \nu$ . However, relativistic corrections produce a constructive contribution to the  $B_c \rightarrow \gamma \ell \bar{\nu}$ . Our results demonstrate that the QCD and relativistic corrections are mandatory toward a more accurate extraction of the value of LDMEs for  $B_c$  system.

## 5 Summary

In this work, we have analyzed the radiative leptonic  $B_c \rightarrow \gamma \ell \bar{\nu}$  decays in the NRQCD effective field theory. NRQCD factorization ensures the separation of short-distance and long-distance effects of  $B_c \rightarrow \gamma \ell \bar{\nu}$  to all orders of  $\alpha_s$ . Treating the photon as a hard object whose interactions with the heavy quarks can be integrated out, we arrive at a factorization formula for the decay amplitude.

We have calculated not only the short-distance coefficients at leading order and next-to-leading order in  $\alpha_s$ , but also the nonrelativistic corrections at the order  $|\mathbf{v}|^2$  in our analysis. We found that the QCD corrections can significantly

**Table 1** Branching ratios of  $B_c \rightarrow \ell \nu$ . Here and in the following table  $\tau_{B_c} = 0.50$  ps, and we vary the heavy quark masses with  $m_b = 4.8 \pm 0.1$  GeV and  $m_c = 1.5 \pm 0.1$  GeV. For the relativistic corrections, we adopt  $\langle v^2 \rangle_{B_c} \simeq 0.186$ 

Channels	Tree-level	$ v ^2$ -corrections	QCD corrections	NLO
$B_c \rightarrow \tau \bar{\nu}_\tau$	$2.90 \times 10^{-2}$	$-0.54 \times 10^{-2}$	$-0.56_{-0.04}^{+0.03} \times 10^{-2}$	$1.80_{-0.04}^{+0.03} \times 10^{-2}$
$B_c \rightarrow \mu \bar{\nu}_\mu$	$12.10 \times 10^{-5}$	$-2.25 \times 10^{-5}$	$-2.32_{-0.16}^{+0.14} \times 10^{-5}$	$7.53_{-0.16}^{+0.14} \times 10^{-5}$
$B_c \rightarrow e \bar{\nu}_e$	$2.82 \times 10^{-9}$	$-0.53 \times 10^{-9}$	$-0.54_{-0.04}^{+0.03} \times 10^{-9}$	$1.75_{-0.04}^{+0.03} \times 10^{-9}$

**Table 2** Branching ratios of  $B_c \rightarrow \gamma \ell \bar{\nu}$ . Here we adopt three cut conditions for photon energy, i.e.  $E_k \geq 0.25$  GeV in Cut-I,  $E_k \geq 0.5$  GeV in Cut-II, and  $E_k \geq 1$  GeV in Cut-III

Channels	Tree-level	$ v ^2$ -corrections	QCD corrections	NLO
Cut-I	$10.30_{-1.77}^{+2.23} \times 10^{-5}$	$5.24_{-1.03}^{+1.30} \times 10^{-5}$	$-7.79_{-1.57}^{+1.96} \times 10^{-5}$	$7.75_{-1.23}^{+1.57} \times 10^{-5}$
Cut-II	$9.77_{-1.68}^{+2.12} \times 10^{-5}$	$4.86_{-0.95}^{+1.20} \times 10^{-5}$	$-7.57_{-1.48}^{+1.37} \times 10^{-5}$	$7.06_{-1.15}^{+1.41} \times 10^{-5}$
Cut-III	$7.97_{-1.80}^{+1.72} \times 10^{-5}$	$3.83_{-0.75}^{+0.95} \times 10^{-5}$	$-6.44_{-1.27}^{+1.57} \times 10^{-5}$	$5.36_{-0.85}^{+1.10} \times 10^{-5}$

**Table 3** Branching ratios of  $B_c \rightarrow \gamma \ell \bar{\nu}$  and  $B_c \rightarrow \ell \nu$  compared with other theories or models, including Lattice QCD (LQCD), Light front model (LFM), Constituent quark model (CQM). Here  $\tau_{B_c} = 0.50$  ps is adopted and we use the cut-I result for comparison

	This work	LQCD [75]	LFM [56]	CQM [58]	NRQCD [66]	Ref. [55]
$10^2 B(B_c \rightarrow \tau \bar{\nu}_\tau)$	$1.80_{-0.04}^{+0.03}$	2.12	1.52	1.44	1.8	1.6
$10^5 B(B_c \rightarrow \mu \bar{\nu}_\mu)$	$7.53_{-0.16}^{+0.14}$	8.86	6.09	6.2	7.6	5.7
$10^9 B(B_c \rightarrow e \bar{\nu}_e)$	$1.75_{-0.04}^{+0.03}$	2.06	1.41	1.47	1.7	1.5
$10^5 B(B_c \rightarrow \gamma \mu \bar{\nu}_\mu)$	$7.75_{-1.23}^{+1.57}$	—	2.2 (5)	4.71	—	4.78

decrease the branching ratio, which has a very important impact on extracting the long-distance operator matrix elements of  $B_c$ . For phenomenological applications, we have estimated the long-distance matrix elements, which are further used to explore the photon energy, lepton energy, and lepton-neutrino invariant mass distribution. These results can be examined at the LHCb experiment.

**Acknowledgments** We are grateful to Prof. Yu Jia, Cong-Feng Qiao, Cai-Dian Lü, and Dr. Si-Hong Zhou for fruitful discussions. We are thankful for the support of a key laboratory grant from the Office of Science and Technology, Shanghai Municipal Government (No. 11DZ2260700), and by Shanghai Natural Science Foundation under Grant No. 15ZR1423100.

**Open Access** This article is distributed under the terms of the Creative Commons Attribution 4.0 International License (<http://creativecommons.org/licenses/by/4.0/>), which permits unrestricted use, distribution, and reproduction in any medium, provided you give appropriate credit to the original author(s) and the source, provide a link to the Creative Commons license, and indicate if changes were made. Funded by SCOAP<sup>3</sup>.

## Appendix A: Ward identities for matrix elements

In this section, following Ref. [69] we will explicitly derive the constraints on the  $B_c \rightarrow \gamma$  form factors arising from

a Ward identity for the conservation of the electromagnetic current. To be more specific, let us consider the following matrix element:

$$\langle \gamma(k, \epsilon) | (\bar{c} \gamma_\nu \gamma_5 b)(0) | \bar{B}_c \rangle = i e \epsilon^{\mu} \int d^4 x e^{i k \cdot x} \langle 0 | T j_\mu^{e.m.}(x) (\bar{c} \gamma_\nu \gamma_5 b)(0) | \bar{B}_c \rangle. \quad (A1)$$

In this case, the electromagnetic current includes contributions from heavy quarks  $j_\mu^{e.m.} = e_c \bar{c} \gamma_\mu c + e_b \bar{b} \gamma_\mu b$ .

The conservation of the electromagnetic current implies a Ward identity for the matrix element of the time-ordered product in (A1),

$$\begin{aligned} i k^\mu \int d^4 x e^{i k \cdot x} \langle 0 | T j_\mu^{e.m.}(x) | (\bar{c} \gamma_\nu \gamma_5 b)(0) | \bar{B}_c \rangle \\ = \int d^3 x e^{i k \cdot x} (\langle 0 | j_0^{e.m.}(x) (\bar{c} \gamma_\nu \gamma_5 b)(0) | \bar{B}_c \rangle \theta(x^0) \\ + \langle 0 | (\bar{c} \gamma_\nu \gamma_5 b)(0) j_0^{e.m.}(x) | \bar{B}_c \rangle \theta(-x^0)) \Big|_{x^0 \rightarrow -\infty}^{x^0 \rightarrow \infty} \\ = \int d^3 x e^{-i \vec{k} \cdot \vec{x}} (\langle 0 | j_0^{e.m.}(\vec{x}) (\bar{c} \gamma_\nu \gamma_5 b)(0) | \bar{B}_c \rangle \\ - \langle 0 | (\bar{c} \gamma_\nu \gamma_5 b)(0) j_0^{e.m.}(\vec{x}) | \bar{B}_c \rangle) \\ = \int d^3 x e^{-i \vec{k} \cdot \vec{x}} \langle f | [j_0^{e.m.}(\vec{x}), (\bar{c} \gamma_\nu \gamma_5 b)(\vec{0})] | \bar{B}_c \rangle. \quad (A2) \end{aligned}$$

The commutator on the right-hand side is non-vanishing, since the operator  $\bar{c}\gamma_\nu\gamma_5b$  carries an electric charge. It can be evaluated as

$$\begin{aligned} & \int d^3x e^{-i\vec{k}\cdot\vec{x}} \langle 0 | [j_0^{\text{e.m.}}(\vec{x}), (\bar{c}\gamma_\nu\gamma_5b)(\vec{0})] | \bar{B}(p_{B_c}) \rangle \\ &= \int d^3x e^{-i\vec{k}\cdot\vec{x}} \langle 0 | [e_c c_m^\dagger(\vec{x}) c_m(\vec{x}) \\ &+ e_b b_m^\dagger(\vec{x}) b_m(\vec{x}), c_n^\dagger(0) (\gamma^0 \gamma_\nu \gamma_5)_{ns} b_s(0)] | \bar{B}(p_{B_c}) \rangle \\ &= (e_c - e_b) \langle 0 | (\bar{c}\gamma_\nu\gamma_5b)(\vec{0}) | \bar{B}_c(p_{B_c}) \rangle \\ &= i(e_c - e_b) f_{B_c} p_{B_c, \nu}. \end{aligned} \quad (\text{A3})$$

The most general parametrization of the matrix element on the left-hand side without  $k^\mu$  can be written in terms of five form factors  $f_i(k^2, p_{B_c} \cdot k)$ ,

$$\begin{aligned} & i \int d^4x e^{ik \cdot x} \langle 0 | T j_\mu^{\text{e.m.}}(x) (\bar{c}\gamma_\nu\gamma_5b)(0) | \bar{B}_c \rangle \\ &= i [f_1 g_{\mu\nu} + f_2 p_{B_c, \mu} p_{B_c, \nu} + f_3 k_\mu k_\nu \\ &+ f_4 k_\mu p_{B_c, \nu} + f_5 p_{B_c, \mu} k_\nu]. \end{aligned} \quad (\text{A4})$$

The Ward identity (A3) implies two constraints on these form factors,

$$\begin{aligned} (p_{B_c} \cdot k) f_2 + k^2 f_4 &= (e_c - e_b) f_{B_c}, \\ f_1 + k^2 f_3 + (p_{B_c} \cdot k) f_5 &= 0. \end{aligned} \quad (\text{A5})$$

For a real photon,  $k^2 = 0$ , these constraints fix uniquely the form factor  $f_2(0, p_{B_c} \cdot k)$ , and relate  $f_1(0, p_{B_c} \cdot k)$  and  $f_5(0, p_{B_c} \cdot k)$ , which leads to

$$\begin{aligned} \langle \gamma(\epsilon, k) | \bar{c}\gamma_\mu\gamma_5b | \bar{B}_c(p_{B_c}) \rangle &= i e p_{B_c} \cdot k f_5 \left( \epsilon_\mu^* - k_\mu \frac{p_{B_c} \cdot \epsilon^*}{p_{B_c} \cdot k} \right) \\ &- \frac{i e}{p_{B_c} \cdot k} f_{B_c} p_{B_c, \mu} p_{B_c} \cdot \epsilon^*. \end{aligned} \quad (\text{A6})$$

This is the same as the result in Eq. (9) as presented in the text, with the identification  $p_{B_c} \cdot k f_5 = A$ .

## Appendix B: Passarino–Veltman integrals

The coefficients  $b_i$ ,  $c_i$ , and  $d_i$  are related to the scalar Passarino–Veltman integrals defined in Refs. [76, 77], and we have split the finite pieces  $b_i = B_i^{\text{finite}}$ ,  $c_i = C_i^{\text{finite}}/m_b^2$ , and  $d_i = D_i^{\text{finite}}/m_b^4$ :

$$\begin{aligned} B_1 &= B_0(0, z^2 m_b^2, z^2 m_b^2), \\ B_2 &= B_0(0, m_b^2, m_b^2), \\ B_3 &= B_0(m_b^2(y^2 - z\bar{z})/\bar{z}, 0, m_b^2), \\ B_4 &= B_0(y^2 m_b^2, m_b^2, z^2 m_b^2), \\ C_1 &= C_0(m_b^2, 0, m_b^2(y^2 - z\bar{z})/\bar{z}, 0, m_b^2, m_b^2), \\ C_2 &= C_0(\bar{z}^2 m_b^2, y^2 m_b^2, 0, m_b^2, z^2 m_b^2, m_b^2), \end{aligned}$$

$$\begin{aligned} C_3 &= C_0(m_b^2, z^2 m_b^2, \bar{z}^2 m_b^2, m_b^2, 0, z^2 m_b^2), \\ C_4 &= C_0(m_b^2(y^2 - z\bar{z})/\bar{z}, m_b^2 y^2, m_b^2 z^2, 0, m_b^2, m_b^2 z^2), \\ D_1 &= D_0(m_b^2, z^2 m_b^2, y^2 m_b^2, 0, \bar{z}^2 m_b^2, m_b^2(y^2 - z\bar{z})/\bar{z}, m_b^2, 0, z^2 m_b^2, m_b^2). \end{aligned} \quad (\text{B1})$$

Here we give the results of the divergence integrals:

$$\begin{aligned} B_1 &= \frac{1}{\epsilon_{\text{UV}}} + \ln \frac{\mu^2}{z^2 m_b^2}, \\ B_2 &= \frac{1}{\epsilon_{\text{UV}}} + \ln \frac{\mu^2}{m_b^2}, \\ B_3 &= \frac{1}{\epsilon_{\text{UV}}} + \ln \frac{\mu^2}{m_b^2} - \frac{(y^2 - \bar{z}^2) \ln(\bar{z} - \frac{y^2}{\bar{z}})}{y^2 - z\bar{z}} + 2, \\ B_4 &= \frac{1}{\epsilon_{\text{UV}}} + \ln \frac{\mu^2}{y^2 m_b^2} + 2 + \sum_{i=1}^2 (\gamma_i(y) \ln \left( \frac{\gamma_i(y) - 1}{\gamma_i(y)} \right) \\ &- \ln(\gamma_i(y) - 1)), \\ C_3 &= -\frac{1}{2z m_b^2} \left( \frac{1}{\epsilon_{\text{IR}}} + t_1 + \ln \frac{\mu^2}{m_b^2} - 2 - \frac{2 \ln z}{1+z} \right), \\ D_1 &= \frac{\bar{z}}{2m_b^4 z (\bar{z}^2 - y^2)} \left( \frac{1}{\epsilon_{\text{IR}}} + t_1 + \ln \frac{\mu^2}{m_b^2} - 2 \ln \frac{\bar{z}^2 - y^2}{\bar{z}} \right. \\ &+ \frac{1}{(y - \bar{z})(y + \bar{z})} (2(\bar{z}^2 - 2y^2 \ln y - (y^2 + z^2 - 1) \ln z \\ &- y^2(1 + 2 \ln 2)) + (-g_5 + y^2 + z^2 - 1) g_1 \\ &+ (g_5 + y^2 - z^2 + 1) g_2 + (-g_5 + y^2 - z^2 + 1) g_3 \\ &\left. + (g_5 + y^2 + z^2 - 1) g_4 \right), \end{aligned} \quad (\text{B2})$$

where

$$\begin{aligned} \gamma_{1,2}(x) &= \frac{\pm \sqrt{(x^2 - z^2 + 1)^2 - 4x^2 + x^2 - z^2 + 1}}{2x^2}, \\ g_1 &= \ln \left( \sqrt{(y^2 - z^2 + 1)^2 - 4y^2} - y^2 - z^2 + 1 \right), \\ g_2 &= \ln \left( \sqrt{(y^2 - z^2 + 1)^2 - 4y^2} + y^2 - z^2 + 1 \right), \\ g_3 &= \ln \left( -\sqrt{(y^2 - z^2 + 1)^2 - 4y^2} + y^2 - z^2 + 1 \right), \\ g_4 &= \ln \left( -\sqrt{(y^2 - z^2 + 1)^2 - 4y^2} - y^2 - z^2 + 1 \right), \\ g_5 &= \sqrt{y^4 - 2y^2(z^2 + 1) + (z^2 - 1)^2}. \end{aligned} \quad (\text{B3})$$

## Appendix C: One-loop corrections to the axial-vector form factor A

The most general structure of the matrix element of the axial-vector current is parametrized by

$$\langle \gamma(\epsilon, k) | \bar{c} \gamma_\mu \gamma_5 b | [\bar{c} b(^1S_0^{[1]})] \rangle = ie \left( \epsilon_\mu^* \mathbb{A}^\epsilon - k_\mu \frac{p_{B_c} \cdot \epsilon^*}{p_{B_c} \cdot k} \mathbb{A}^k \right) - ie \frac{p_{B_c} \cdot \epsilon^*}{p_{B_c} \cdot k} \mathcal{V}^A p_{B_c \mu}. \quad (\text{C1})$$

This section will be devoted to a demonstration of the gauge invariance at the one-loop level in  $\alpha_s$ , namely

$$\mathbb{A}^\epsilon = \mathbb{A}^k \equiv \mathbb{A}, \quad (\text{C2})$$

$$\mathcal{V}^A = \mathcal{V}. \quad (\text{C3})$$

The contributions from individual diagrams to  $\mathbb{A}^\epsilon$  are given by

$$\begin{aligned} \mathbb{A}_b^\epsilon = & \frac{e_b C_F \alpha_s \sqrt{2N_c}}{4\pi m_b} \left[ \frac{1}{\hat{\epsilon}_{\text{IR}}} - \frac{4(z-1)\tilde{z}^2}{(y^2 - \tilde{z}^2)^2} \right. \\ & + \frac{y^2 \tilde{z}^2 - 2(z-1)\tilde{z}^3 - y^4}{(y^2 - \tilde{z}^2)^2 \tilde{z}} b_1 + \frac{y^2}{(y^2 - \tilde{z}^2) \tilde{z}} b_2 \\ & + \frac{2y^2 \tilde{z} - y^4 + (z^2 - 1)^2}{z(y^2 - \tilde{z}^2)^2} b_3 + \frac{-2y^2 \tilde{z} + (z-1)\tilde{z}^3 + y^4}{z(y^2 - \tilde{z}^2)^2} b_4 \\ & - \frac{2(3z-1)\tilde{z}^2 + y^4 - y^2(z^2 + 4z + 3)}{(\tilde{z}^2 - y^2) \tilde{z}} c_4 \\ & \left. - \frac{(z^2 - 1)(y^2 - z^2 + 1)}{(y^2 - \tilde{z}^2) \tilde{z}} c_3 + (-y^2 + z^2 + 4z - 1) d_1 \right], \quad (\text{C4}) \end{aligned}$$

$$\begin{aligned} \mathbb{A}_c^\epsilon = & \frac{e_b C_F \alpha_s \sqrt{2N_c}}{4\pi m_b} \left[ \frac{1}{2} \frac{1}{\hat{\epsilon}_{\text{UV}}} + \frac{\tilde{z} + y^2}{y^2 - \tilde{z}^2} b_1 \right. \\ & + \frac{-y^2(2z+3) + 2z^3 + 5z^2 + 2z - 1}{2z(\tilde{z}^2 - y^2)} b_3 \\ & + \frac{y^2 + z^2 + 4z + 3}{y^2 - \tilde{z}^2} + \frac{\tilde{z}(-3y^2 + z^2 - 1)}{2z(y^2 - \tilde{z}^2)} b_4 \\ & \left. + (-y^2 + z^2 + z - 1) c_4 \right], \quad (\text{C5}) \end{aligned}$$

$$\begin{aligned} \mathbb{A}_d^\epsilon = & \frac{e_b C_F \alpha_s \sqrt{2N_c}}{4\pi m_b} \left[ \frac{1}{2} \frac{1}{\hat{\epsilon}_{\text{UV}}} + \frac{y^2 - z^2 + 1}{y^2 - \tilde{z}^2} + \frac{y^2 - z\tilde{z}}{y^2 - \tilde{z}^2} b_2 \right. \\ & \left. + -\frac{y^2 - z^2 + 1}{2(y^2 - \tilde{z}^2)} b_3 - \tilde{z} c_1 \right], \quad (\text{C6}) \end{aligned}$$

$$\begin{aligned} \mathbb{A}_e^\epsilon = & \frac{e_b C_F \alpha_s \sqrt{2N_c}}{4\pi m_b} \left[ -\frac{1}{2\hat{\epsilon}_{\text{UV}}} + \frac{y^2 - z^2 + 1}{2(y^2 - z\tilde{z})} + \frac{\tilde{z}}{2y^2 - 2z\tilde{z}} b_2 \right. \\ & \left. - \frac{y^2 - z^2 + 1}{2(y^2 - z\tilde{z})} b_3 \right]. \quad (\text{C7}) \end{aligned}$$

The mass counter-term and wave function renormalization give the contributions:

$$\begin{aligned} \mathbb{A}_{\text{CT}-m}^\epsilon &= 0, \\ \mathbb{A}_{\text{CT}-F}^\epsilon &= -\mathcal{V}_{\text{CT}-F}. \quad (\text{C8}) \end{aligned}$$

The contributions from individual diagrams to  $\mathbb{A}^k$  are given as

$$\begin{aligned} \mathbb{A}_b^k = & \frac{e_b C_F \alpha_s \sqrt{2N_c}}{4\pi m_b} \\ & \times \left[ -\frac{\tilde{z}(y^2(-7z^2 + 10z + 1)\tilde{z}^2 + (z-1)\tilde{z}^5 + y^4(3y^2 + 3z^2 - 8z - 11))}{(y^2 - z\tilde{z})(y^3 - y\tilde{z}^2)^2} \right. \\ & + \frac{2y^2(3-2z)\tilde{z}^2 + z\tilde{z}^4 + y^4(-(z+2))}{(y^3 - y\tilde{z}^2)^2} b_1 \\ & + \frac{\tilde{z} + y^2}{y^4 - y^2 z\tilde{z}} b_2 - \frac{2\tilde{z}(-y^2 + z^2 + 3)}{(y^2 - \tilde{z}^2)} c_4 \\ & + \frac{-y^2 \tilde{z}^2(y^2 + z^2 - 4z + 5) + (z^3 - 3z^2 + 5z + 1)\tilde{z}^3 + y^6}{z(-y^2 + z^2 + z)(y^2 - \tilde{z}^2)^2} b_3 \\ & \left. + \frac{y^2(3z-5)\tilde{z}^3 - (z-1)\tilde{z}^5 + y^4(y^2 + z^2 - 1)}{z(y^3 - y\tilde{z}^2)^2} b_4 \right] + \mathbb{A}_b^\epsilon, \quad (\text{C9}) \end{aligned}$$

$$\begin{aligned} \mathbb{A}_c^k = & \frac{e_b C_F \alpha_s \sqrt{2N_c}}{4\pi m_b} \\ & \times \left[ \frac{\tilde{z}(y^2(-7z^2 + 10z + 1)\tilde{z}^2 + (z-1)\tilde{z}^5 + y^4(3y^2 + 3z^2 - 8z - 11))}{(y^2 - z\tilde{z})(y^3 - y\tilde{z}^2)^2} \right. \\ & + \frac{2y^2(2z-3)\tilde{z}^2 - z\tilde{z}^4 + y^4(z+2)}{(y^3 - y\tilde{z}^2)^2} b_1 \\ & + \frac{\tilde{z} + y^2}{y^4 - y^2 z\tilde{z}} b_2 - \frac{2\tilde{z}(-y^2 + z^2 + 3)}{(y^2 - \tilde{z}^2)} c_4 \\ & - \frac{-y^2 \tilde{z}^2(y^2 + z^2 - 4z + 5) + (z^3 - 3z^2 + 5z + 1)\tilde{z}^3 + y^6}{z(z\tilde{z} - y^2)(y^2 - \tilde{z}^2)^2} b_3 \\ & \left. - \frac{y^2(3z-5)\tilde{z}^3 - (z-1)\tilde{z}^5 + y^4(y^2 + z^2 - 1)}{z(y^3 - y\tilde{z}^2)^2} b_4 \right] + \mathbb{A}_c^\epsilon, \quad (\text{C10}) \end{aligned}$$

$$\begin{aligned} \mathbb{A}_d^k = & \mathbb{A}_d^\epsilon + \frac{e_b C_F \alpha_s \sqrt{2N_c}}{4\pi m_b} \left[ \frac{\tilde{z}(5y^2 - 5z^2 - 6z - 1)}{(y^2 - \tilde{z}^2)(y^2 - z\tilde{z})} \right. \\ & + \frac{\tilde{z}(3y^2 - 3z^2 - 4z - 1)}{(y^2 - \tilde{z}^2)(y^2 - z\tilde{z})} b_2 \\ & \left. + \frac{\tilde{z}(-3y^2 + 3z^2 + 4z + 1)}{(y^2 - \tilde{z}^2)(y^2 - z\tilde{z})} b_3 \right], \quad (\text{C11}) \end{aligned}$$

$$\begin{aligned} \mathbb{A}_e^k = & \mathbb{A}_e^\epsilon + \frac{e_b C_F \alpha_s \sqrt{2N_c}}{4\pi m_b} \left[ \frac{3\tilde{z}}{y^2 - \tilde{z}^2} \frac{1}{\hat{\epsilon}_{\text{UV}}} + \frac{\tilde{z}}{-y^2 + z^2 + z} \right. \\ & \left. + \frac{\tilde{z}^2}{(y^2 - \tilde{z}^2)(y^2 - z\tilde{z})} b_2 + \frac{\tilde{z}(3y^2 - 3z^2 - 4z - 1)}{(y^2 - \tilde{z}^2)(y^2 - z\tilde{z})} b_3 \right]. \quad (\text{C12}) \end{aligned}$$

Similar, the mass counter-terms and wave function renormalization corrections give

$$\begin{aligned} \mathbb{A}_{\text{CT}-m}^k &= \frac{e_b C_F \alpha_s \sqrt{2N_c}}{4\pi m_b} \left[ \frac{3\tilde{z}}{\tilde{z}^2 - y^2} \left( \frac{1}{\hat{\epsilon}_{\text{UV}}} + \ln \frac{\mu^2}{m_b^2} + \frac{4}{3} \right) \right], \\ \mathbb{A}_{\text{CT}-F}^k &= \mathbb{A}_{\text{CT}-F}^\epsilon. \quad (\text{C13}) \end{aligned}$$

Adding the above contributions, one may derive the relation  $\mathbb{A}^\epsilon = \mathbb{A}^k$ , which is guaranteed by gauge invariance. One can obtain the one-loop results for  $\mathbb{A}$  by adding up the anti-symmetrical part with  $e_b \rightarrow e_c$  and  $m_b \leftrightarrow m_c$ .

The contributions from individual diagrams to  $\mathcal{U}^A$  are given as

$$\mathcal{U}_b^A = \frac{e_b C_F \alpha_s \sqrt{2N_c}}{4\pi} \left[ -\frac{2}{\hat{\epsilon}_{\text{IR}}} + \frac{y^2(3z^2 - 6z - 1)\tilde{z}^2 - (z - 1)\tilde{z}^5 + y^4(-3y^2 + z^2 + 8z + 7)}{y^2(y^2 - \tilde{z}^2)(y^2 - z\tilde{z})} + \frac{-3y^2(z - 1)\tilde{z}^2 + z\tilde{z}^4 - y^4}{y^2\tilde{z}(y^2 - \tilde{z}^2)} b_1 + \frac{-(y^4 + 3)z + (y^2 - 1)z^3 + (y^2 - 3)z^2 - 1}{y^2\tilde{z}(y^2 - z\tilde{z})} b_2 + \frac{4y^2\tilde{z} + (z^2 - 4z - 1)\tilde{z}^2 - y^4}{z(y^2 - \tilde{z}^2)(y^2 - z\tilde{z})} b_3 + \frac{\tilde{z}(-(z - 1)\tilde{z}^3 + y^4 + 2y^2(z^2 - z - 2))}{y^2z(y^2 - \tilde{z}^2)} b_4 - 2\tilde{z}c_4 + 4z c_3 \right], \quad (\text{C14})$$

$$\mathcal{U}_c^A = \frac{e_b C_F \alpha_s \sqrt{2N_c}}{4\pi} \left[ -\frac{1}{\hat{\epsilon}_{\text{UV}}} + \frac{y^2(-5z^2 + 4z + 1)\tilde{z}^2 + (z - 1)\tilde{z}^5 + y^4(y^2 + 3z^2 - 2z - 5)}{y^2(y^2 - \tilde{z}^2)(y^2 - z\tilde{z})} - \frac{\tilde{z}(z\tilde{z}^2 + y^2(2 - 3z))}{y^4 - y^2\tilde{z}^2} b_1 + \frac{\tilde{z}^2}{y^4 - y^2z\tilde{z}} b_2 + \frac{-4y^2\tilde{z} + (-z^2 + 4z + 1)\tilde{z}^2 + y^4}{z(y^2 - \tilde{z}^2)(y^2 - z\tilde{z})} b_3 + \frac{\tilde{z}((z - 1)\tilde{z}^3 - y^2(y^2 + 2z^2 - 2z - 4))}{y^2z(y^2 - \tilde{z}^2)} b_4 + 2\tilde{z}c_4 \right], \quad (\text{C15})$$

$$\mathcal{U}_d^A = \frac{e_b C_F \alpha_s \sqrt{2N_c}}{4\pi} \left[ -\frac{1}{\hat{\epsilon}_{\text{UV}}} + \frac{(z^2 + 10z + 1)\tilde{z}^2 + y^4 - 2y^2(z^2 + 6z + 5)}{(y^2 - \tilde{z}^2)(y^2 - z\tilde{z})} + \frac{\tilde{z}(-5y^2 + 5z^2 + 6z + 1)}{(y^2 - \tilde{z}^2)(y^2 - z\tilde{z})} b_2 - \frac{(z^2 + 6z + 1)\tilde{z}^2 + y^4 - 2y^2(z^2 + 4z + 3)}{(y^2 - \tilde{z}^2)(y^2 - z\tilde{z})} b_3 \right], \quad (\text{C16})$$

$$\mathcal{U}_e^A = \frac{e_b C_F \alpha_s \sqrt{2N_c}}{4\pi} \left[ \frac{y^2 - z^2 - 8z - 7}{y^2 - \tilde{z}^2} \frac{1}{\hat{\epsilon}_{\text{UV}}} + \frac{\tilde{z}^2 - y^2}{y^2 - z\tilde{z}} + \frac{\tilde{z}(-y^2 + z^2 - 1)}{(y^2 - \tilde{z}^2)(y^2 - z\tilde{z})} b_2 + \frac{(z^2 + 6z + 1)\tilde{z}^2 + y^4 - 2y^2(z^2 + 4z + 3)}{(y^2 - \tilde{z}^2)(y^2 - z\tilde{z})} b_3 \right], \quad (\text{C17})$$

$$\mathcal{U}_{\text{CT}-m}^A = -\frac{2}{\tilde{z}} \mathbb{A}_{\text{CT}-m}^\epsilon, \quad \mathcal{U}_{\text{CT}-F}^A = -\frac{2}{\tilde{z}} \mathbb{A}_{\text{CT}-F}^\epsilon. \quad (\text{C18})$$

The sum of them is

$$\mathcal{U}_{b-e+\text{CT}}^A = -\frac{3e_b C_F \alpha_s \sqrt{2N_c} ((z - 1) \ln(z) - 2\tilde{z} + 2/3t_1)}{4\pi \tilde{z}}. \quad (\text{C19})$$

We can get the one-loop result in Eq. 60 after adding up the symmetrical part with  $e_b \rightarrow e_c$  and  $m_b \leftrightarrow m_c$ .

## References

- W. Wang, Int. J. Mod. Phys. A **29**, 1430040 (2014). [arXiv:1407.6868](#) [hep-ph]
- N. Brambilla et al. (Quarkonium Working Group Collaboration), [arXiv:hep-ph/0412158](#)
- N. Brambilla, S. Eidelman, B.K. Heltsley, R. Vogt, G.T. Bodwin, E. Eichten, A.D. Frawley, A.B. Meyer et al., Eur. Phys. J. C **71**, 1534 (2011). [arXiv:1010.5827](#) [hep-ph]
- F. Abe et al. (CDF Collaboration), Phys. Rev. Lett. **81**, 2432 (1998). [arXiv:hep-ex/9805034](#)
- R. Aaij et al. (LHCb Collaboration), Phys. Lett. B **742**, 29 (2015). [arXiv:1411.6899](#) [hep-ex]
- R. Aaij et al. (LHCb Collaboration), Eur. Phys. J. C **74**, 2839 (2014)
- R. Aaij et al. (LHCb Collaboration), Phys. Rev. D **90**, 032009 (2014)
- R. Aaij et al. (LHCb Collaboration), Phys. Rev. Lett. **114**, 132001 (2015). [arXiv:1411.2943](#) [hep-ex]
- R. Aaij et al. (LHCb Collaboration), JHEP **1405**, 148 (2014)
- R. Aaij et al. (LHCb Collaboration), Phys. Rev. Lett. **113**, 152003 (2014)
- R. Aaij et al. (LHCb Collaboration), JHEP **1309**, 075 (2013)
- R. Aaij et al. (LHCb Collaboration), Phys. Rev. D **87**, 071103 (2013)
- R. Aaij et al. (LHCb Collaboration), Eur. Phys. J. C **73**(4), 2373 (2013)
- (ATLAS Collaboration), ATLAS-CONF-2012-028, ATLAS-COM-CONF-2012-035
- V. Khachatryan et al. (CMS Collaboration), JHEP **1501**, 063 (2015). [arXiv:1410.5729](#) [hep-ex]
- D.S. Du, Z. Wang, Phys. Rev. D **39**, 1342 (1989)
- P. Colangelo, G. Nardulli, N. Paver, Z. Phys. C **57**, 43 (1993)
- V.V. Kiselev, A.V. Tkabladze, Phys. Rev. D **48**, 5208 (1993)
- D. Choudhury, A. Kundu, B. Mukhopadhyaya, [arXiv:hep-ph/9810339](#)
- V.V. Kiselev, A.K. Likhoded, A.I. Onishchenko, Nucl. Phys. B **569**, 473 (2000)
- M.A. Nobes, R.M. Woloshyn, J. Phys. G **26**, 1079 (2000)
- M.A. Ivanov, J.G. Korner, P. Santorelli, Phys. Rev. D **63**, 074010 (2001)
- V.V. Kiselev, [arXiv:hep-ph/0211021](#)
- D. Ebert, R.N. Faustov, V.O. Galkin, Phys. Rev. D **68**, 094020 (2003)
- D. Ebert, R.N. Faustov, V.O. Galkin, Eur. Phys. J. C **32**, 29 (2003)
- J.F. Sun, D.S. Du, Y.L. Yang, Eur. Phys. J. C **60**, 107 (2009). [arXiv:0808.3619](#) [hep-ph]
- F. Zuo, T. Huang, Chin. Phys. Lett. **24**, 61 (2007). [arXiv:hep-ph/0611113](#)
- M.A. Ivanov, J.G. Korner, P. Santorelli, Phys. Rev. D **71**, 094006 (2005). [arXiv:hep-ph/0501051](#) [Erratum-ibid. D **75**, 019901 (2007)]
- W. Wang, Y.L. Shen, C.D. Lu, Eur. Phys. J. C **51**, 841 (2007). [arXiv:0704.2493](#) [hep-ph]
- Y.M. Wang, C.D. Lu, Phys. Rev. D **77**, 054003 (2008). [arXiv:0707.4439](#) [hep-ph]
- T.M. Aliev, M. Savci, Eur. Phys. J. C **47**, 413 (2006). [arXiv:hep-ph/0601267](#)
- E. Hernandez, J. Nieves, J.M. Verde-Velasco, Phys. Rev. D **74**, 074008 (2006). [arXiv:hep-ph/0607150](#)
- T. Huang, F. Zuo, Eur. Phys. J. C **51**, 833 (2007). [arXiv:hep-ph/0702147](#) [HEP-PH]
- R. Dhir, N. Sharma, R.C. Verma, J. Phys. G **35**, 085002 (2008)
- R.C. Verma, A. Sharma, Phys. Rev. D **65**, 114007 (2002)
- R. Dhir, R.C. Verma, Phys. Rev. D **79**, 034004 (2009). [arXiv:0810.4284](#) [hep-ph]

37. W. Wang, Y.L. Shen, C.D. Lu, Phys. Rev. D **79**, 054012 (2009). [arXiv:0811.3748](#) [hep-ph]
38. X.X. Wang, W. Wang, C.D. Lu, Phys. Rev. D **79**, 114018 (2009). [arXiv:0901.1934](#) [hep-ph]
39. C.F. Qiao, R.L. Zhu, Phys. Rev. D **87**, 014009 (2013). [arXiv:1208.5916](#) [hep-ph]
40. W.F. Wang, Y.Y. Fan, Z.J. Xiao, Chin. Phys. C **37**, 093102 (2013)
41. Z. Rui, Z.T. Zou, Phys. Rev. D **90**, 114030 (2014). [arXiv:1407.5550](#) [hep-ph]
42. J.M. Shen, X.G. Wu, H.H. Ma, S.Q. Wang, Phys. Rev. D **90**(3), 034025 (2014). [arXiv:1407.7309](#) [hep-ph]
43. X.G. Wu, C.H. Chang, Y.Q. Chen, Z.Y. Fang, Phys. Rev. D **67**, 094001 (2003). [arXiv:hep-ph/0209125](#)
44. T. Huang, Z.H. Li, X.G. Wu, F. Zuo, Int. J. Mod. Phys. A **23**, 3237 (2008). [arXiv:0801.0473](#) [hep-ph]
45. T. Zhong, X.G. Wu, T. Huang, Eur. Phys. J. C **75**, 45 (2015). [arXiv:1408.2297](#) [hep-ph]
46. C.F. Qiao, P. Sun, D. Yang, R.L. Zhu, Phys. Rev. D **89**(3), 034008 (2014). [arXiv:1209.5859](#) [hep-ph]
47. C.F. Qiao, P. Sun, F. Yuan, JHEP **1208**, 087 (2012). [arXiv:1103.2025](#) [hep-ph]
48. X. Liu, Z.J. Xiao, C.D. Lu, Phys. Rev. D **81**, 014022 (2010). [arXiv:0912.1163](#) [hep-ph]
49. X. Liu, Z.J. Xiao, J. Phys. G **38**, 035009 (2011)
50. Z.J. Xiao, X. Liu, Phys. Rev. D **84**, 074033 (2011). [arXiv:1111.6679](#) [hep-ph]
51. Z.J. Xiao, X. Liu, Chin. Sci. Bull. **59**, 3748 (2014). [arXiv:1401.0151](#) [hep-ph]
52. Z.G. Wang, Phys. Rev. D **86**, 054010 (2012). [arXiv:1205.5317](#) [hep-ph]
53. G.T. Bodwin, E. Braaten, G.P. Lepage, Phys. Rev. D **51**, 1125 (1995). [arXiv:hep-ph/9407339](#) [Erratum-ibid. D **55**, 5853 (1997)]
54. C.H. Chang, J.P. Cheng, C.D. Lu, Phys. Lett. B **425**, 166 (1998). [arXiv:hep-ph/9712325](#)
55. G. Chiladze, A.F. Falk, A.A. Petrov, Phys. Rev. D **60**, 034011 (1999). [arXiv:hep-ph/9811405](#)
56. C.C. Lih, C.Q. Geng, W.M. Zhang, Phys. Rev. D **59**, 114002 (1999)
57. P. Colangelo, F. De Fazio, Mod. Phys. Lett. A **14**, 2303 (1999). [arXiv:hep-ph/9904363](#)
58. C.H. Chang, C.D. Lu, G.L. Wang, H.S. Zong, Phys. Rev. D **60**, 114013 (1999). [arXiv:hep-ph/9904471](#)
59. Y.Y. Charng, H.N. Li, Phys. Rev. D **72**, 014003 (2005). [arXiv:hep-ph/0505045](#)
60. V. Cirigliano, D. Pirjol, Phys. Rev. D **72**, 094021 (2005)
61. M. Beneke, J. Rohrwild, Eur. Phys. J. C **71**, 1818 (2011)
62. V.M. Braun, A. Khodjamirian, Phys. Lett. B **718**, 1014 (2013)
63. B. Aubert et al. (BaBar Collaboration), Phys. Rev. D **80**, 111105 (2009)
64. J. Lee, W. Sang, S. Kim, JHEP **1101**, 113 (2011). [arXiv:1011.2274](#) [hep-ph]
65. A.I. Onishchenko, O.L. Veretin, Eur. Phys. J. C **50**, 801 (2007)
66. L.B. Chen, C.F. Qiao, Phys. Lett. B **748**, 443 (2015). [arXiv:1503.05122](#) [hep-ph]
67. G. Eilam, I.E. Halperin, R.R. Mendel, Phys. Lett. B **361**, 137 (1995). [arXiv:hep-ph/9506264](#)
68. F. Kruger, D. Melikhov, Phys. Rev. D **67**, 034002 (2003). [arXiv:hep-ph/0208256](#)
69. B. Grinstein, D. Pirjol, Phys. Rev. D **62**, 093002 (2000)
70. D. Becirevic, B. Haas, E. Kou, Phys. Lett. B **681**, 257 (2009). [arXiv:0907.1845](#) [hep-ph]
71. Y. Jia, X.T. Yang, W.L. Sang, J. Xu, JHEP **1106**, 097 (2011)
72. E. Braaten, S. Fleming, Phys. Rev. D **52**, 181 (1995). [arXiv:hep-ph/9501296](#)
73. K.A. Olive et al. (Particle Data Group Collaboration), Chin. Phys. C **38**, 090001 (2014)
74. W. Buchmuller, S.H.H. Tye, Phys. Rev. D **24**, 132 (1981)
75. C. McNeile, C.T.H. Davies, E. Follana, K. Hornbostel, G.P. Lepage, Phys. Rev. D **86**, 074503 (2012). [arXiv:1207.0994](#) [hep-lat]
76. G. Passarino, M.J.G. Veltman, Nucl. Phys. B **160**, 151 (1979)
77. T. Hahn, M. Perez-Victoria, Comput. Phys. Commun. **118**, 153 (1999). [arXiv:hep-ph/9807565](#)